

1395770
/410

**SILICON CARBIDE COATINGS BY PLASMA-ENHANCED CHEMICAL
VAPOR DEPOSITION ON SILICON AND POLYIMIDE SUBSTRATES**

**A Thesis Presented to
The Faculty of The Russ College of Engineering and Technology
Ohio University**

**In Partial Fulfillment
of the Requirement for the degree
Master of Science**

**by
Pramod Chakravarthy,
Department of Chemical Engineering
August 1995**

**OHIO UNIVERSITY
LIBRARY**

Thesis
M
1995
CHAK

1395770
/410

Acknowledgements

I would like to express my deep gratitude to my advisor, Dr. Daniel Gulino for his guidance and support in the course of the completion of this study. Thanks are also due to other members of our group; Dr. Larry Miller, Dr. Madan Gopal, Dr. Sudarshan Neogi, Gaurav Dangarwala and Premchand Koganti, for their assistance at various phases of my experimentation.

XPS and AES characterization would not have been possible without the help of Dr. David Ingram of the Edwards Accelerator Laboratory and his students, Sooncheon Seo and Michael Maldei. I would also like to acknowledge Dr. Ingram's suggestions in general regarding thin film characterization. Thanks are also due to Raj Haldankar for his input during the preparation of the manuscript and to Jim McKnight for his contribution in the fabrication of components in the reactor.

Finally, I would like to gratefully acknowledge the system of education in the State of Ohio as well as Ohio's taxpayers for making available the facilities and opportunity for international students like me to pursue higher education in the field of engineering in institutions such as Ohio University.

Table of Contents

Acknowledgements		iii
List of Tables		vi
List of Figures		vii
1.0	Introduction	1
2.0	Literature Review	6
2.1	Deposition of protective films on polyimide composites	7
2.2	Low temperature PECVD of SiC	9
2.3	Tetraethylsilane as a precursor for SiC	13
3.0	Experimental setup and procedure	15
3.1	Process considerations	15
3.2	Precursor considerations	15
3.3	Reactor considerations	16
3.4	Substrate considerations	18
3.5	Post-deposition analysis	19
3.5.1	Profilometry	19
3.5.2	Adhesion strength measurement	20
3.5.3	Weight loss analysis of polyimide composites	21
3.5.4	Electron spectroscopy	21
3.6	Procedures	24
3.6.1	SiC deposition	24
3.6.2	Film thickness and uniformity	25
3.6.3	Film adhesion strength	26

3.6.4	Weight loss experiments	27
3.6.5	Compositional analysis - XPS/AES experiments	28
3.7	Safety considerations	29
4.0	Results and discussion	31
4.1	Thickness measurement	31
4.1.1	Deposition rate versus temperature	31
4.1.2	Deposition rate versus argon flow rate	33
4.1.3	Deposition rate versus temperature	38
4.1.4	Thickness uniformity	40
4.2	Adhesion measurements	42
4.2.1	Adhesion strength versus temperature	42
4.2.2	Adhesion strength versus flow rate	44
4.2.2	Adhesion strength versus film thickness	44
4.3	Composition analysis	47
4.4	Weight loss experiments	61
5.0	Conclusions	69
5.0	Recommendation	71
	References	72
Appendix I	Material Safety Data Sheet for TES	77
Appendix II	Specifications of equipment used	81
Appendix III	Output from XPS analyses	82
Appendix IV	Polyimide composite weight loss data	95

List of Tables

Table I :	PECVD process parameters and data for silicon samples	32
Table II :	Thickness uniformity over 2.25 sq. cm	41
Table A1 :	Polyimide composite weight loss data	95

List of Figures

Figure 1 :	Experimental setup	17
Figure 2 :	A typical AES/XPS experimental setup	23
Figure 3 :	Deposition rate versus Temperature for argon flow rate of 260 ml/min and r.f. power of 100 W	34
Figure 4 :	Deposition rate versus Temperature for argon flow rate of 489 ml/min and r.f. power of 100 W	35
Figure 5 :	Deposition rate versus Temperature for argon flow rate of 718 ml/min and r.f. power of 100 W	36
Figure 6 :	Deposition rate versus Argon flow rate at an r.f. power of 100 W and temperatures of 165, 230, 290 and 350°C	37
Figure 7 :	Deposition rate versus r.f. power at an argon flow rate of 489 ml/min and temperatures of 290 and 350°C	39
Figure 8 :	Adhesion strength versus temperature at flow rates of 260 and 718 ml/min and r.f. power of 100 W	43
Figure 9 :	Adhesion strength versus argon carrier gas flow rate at 350°C and r.f.power of 100 W	45
Figure 10 :	Adhesion strength versus thickness	46
Figure 11 :	Object specifications for a sample AES run	48
Figure 12 :	Screen capture of the object specification menu for a sample AES run	49
Figure 13 :	Object specifications for a sample XPS run	50
Figure 14 :	Screen capture of the object specification menu for a sample XPS run	51
Figure 15 :	XPS survey of a sample with the film made at 300°C, 260 ml/min Ar flow rate and 100 W r.f. power for 15 minutes	53
Figure 16 :	Magnification of the Si 2s peak from the final XPS output for the sample in figure 15	54

Figure 17 :	Magnification of the Si 2p peak from the final XPS output for the sample in figure 15	55
Figure 18 :	Magnification of the C 1s peak from the final XPS output for the sample in figure 15	56
Figure 19 :	Magnification of the O 1s peak from the final XPS output for the sample in figure 15	57
Figure 20 :	Screen capture of a comparative plot of figures 16 through 19	58
Figure 21 :	AES survey of a sample with the film made at 300°C, 260 ml/min Ar flow rate and 100 W r.f. power for 15 minutes. The upper graph indicates a survey before tuning, displaying excessive noise	59
Figure 22 :	Screen capture of the quantification of the data in figures 15 through 21	60
Figure 23 :	Percentage weight loss versus time for two uncoated polyimide composite samples at 375°C	62
Figure 24 :	Percentage weight loss versus time for coated polyimide composite at an ambient temperature of 375°C; coating conditions are: r.f. power = 100W, flow rate = 260 ml/min and temperature = 165, 230, 290 and 350°C	64
Figure 25 :	Percentage weight loss versus time for coated polyimide composite at an ambient temperature of 375°C; coating conditions are: r.f. power = 100W, flow rate = 718 ml/min and temperature = 165, 230, 290 and 350°C	65
Figure 26 :	Percentage improvement in weight loss versus time for coated polyimide composite at an ambient temperature of 375°C; coating conditions are: r.f. power = 100W, flow rate = 260 ml/min and temperature = 165, 230, 290 and 350°C	66
Figure 27 :	Percentage improvement in weight loss versus time for coated polyimide composite at an ambient temperature of 375°C; coating conditions are: r.f. power = 100W, flow rate = 718 ml/min	

and temperature = 165, 230, 290 and 350°C	67
Figure A1 : XPS survey of a sample with the film made at 325°C, 718 ml/min Ar flow rate and 100 W r.f. power for 15 minutes	82
Figure A2 : Magnification of the Si 2s peak from the final XPS output for the sample in figure A1	83
Figure A3 : Magnification of the Si 2p peak from the final XPS output for the sample in figure A1	84
Figure A4 : Magnification of the C 1s peak from the final XPS output for the sample in figure A1	85
Figure A5 : Magnification of the O 1s peak from the final XPS output for the sample in figure A1	86
Figure A6 : Screen capture of a comparative plot of figures A2 through A5	87
Figure A7 : Screen capture of the quantification of the data in figures A1 through A6	88
Figure A8 : XPS survey of a sample with the film made at 350°C, 489 ml/min Ar flow rate and 100 W r.f. power for 30 minutes	89
Figure A9 : Magnification of the Si 2p peak from the final XPS output for the sample in figure A8	90
Figure A10 : Magnification of the C 1s peak from the final XPS output for the sample in figure A8	91
Figure A11 : Magnification of the O 1s peak from the final XPS output for the sample in figure A8	92
Figure A12 : Screen capture of a comparative plot of figures A9 through A11	93
Figure A13 : Screen capture of the quantification of the data in figures A8 through A12	94

1.0 Introduction

The usefulness of polyimide composites as structural materials in aerospace applications, as a substitute for conventional materials, has been studied in recent years in various works. Besides having excellent mechanical properties, the high strength to weight ratio that polyimides possess make them attractive for use in this area. The weight savings that are obtained by the use of composites instead of conventionally used metals have made their use increasingly prevalent in not only aerospace applications, but in the automobile industry as well, due to the improved fuel efficiency arising therefrom. In aerospace applications, the reduction in payload weight is an extremely important quest for designers. In addition, the use of polyimide composites has become attractive due to the fact that in some instances, their mechanical properties exceed those of conventional materials.

Currently, it is estimated that 4% of commercial aircraft and 10% of military aircraft by weight are made up of polyimide composites. In the somewhat more modestly budgeted space station Alpha, the solar arrays will use a commercial polyimide called Kapton[®], which is made by DuPont (Neogi [1992] and Gopal [1991]).

The fundamental problem associated with this material, however, as it is for polymer composites in general, is oxidative degradation at the high temperatures that are likely to be encountered in aerospace applications. Experiments have confirmed this;

polyimide composites degrade completely (the polymer is oxidized and the fiber separated from the matrix) after 100 hours at 425°C in an environment of oxygen. In an environment of nitrogen, however, strength is retained even after 600 hrs at 425°C (Harding [1991]).

It has been shown that coatings of temperature resistant thin films on polyimide surfaces successfully increase the temperature tolerance by preventing oxidation (Harding [1991]). In particular, ceramic material coatings protect the polymer surface from attack by atomic oxygen (ATOX), which is extremely potent due to its existence in a free radical state in low earth orbit (LEO). In this state it is highly reactive and produces stable products, attacking not only organics, but also metals, though with a lesser effect (Neogi [1992] and Gopal [1991]).

The choice of a coating must be based on its ability to prevent oxygen from attacking the polyimide composite resulting in volatilization and delinking of its molecular chains. Application of such a coating should not also result in a significant loss of the inherently favorable mechanical properties of the composite.

Due to the limitation of the temperature that polyimide composites may withstand, it is necessary to design a process whereby coatings may be applied at a temperature below 450°C and, preferably, even lower if the deposition times involved are large. In addition, due to the ultimate application of the coated composite, it is necessary for the

film thus deposited to possess excellent adhesion and resistance to thermal cycling, wear and acoustical vibration. It must also possess the morphology and microstructure to withstand the physical bombardment of particles in low earth orbit as well as the insidious damage that can be caused due to oxygen diffusion that occurs due to atomic oxygen bombardment.

It has been found that, in general, ceramic materials are very resistant to oxidation at high temperatures. In addition, they are hard and chemically inert substances that have been successfully been coated on metals, ceramics and other composites. The Materials Research group at the Department of Chemical Engineering at Ohio University has attempted to deposit and characterize various ceramic coatings on polyimide composites supplied by NASA; among the materials that have been tried as coatings are SiO_2 (Neogi [1992]), Si_3N_4 (Gopal [1991]) and Al_2O_3 (Miller [1991]). A number of techniques have been used based upon the individual properties of the coatings involved and the chemistry of their precursor materials.

In this study, silicon carbide (SiC) thin films are deposited and characterized in order to examine their viability as heat resistant coatings on polyimides. Silicon carbide has already been widely studied as a coating material on silicon and other semiconductor and solar cell materials and has been shown to be a hard, temperature-resistant, and chemically inert substance.

However, there has been very little work done on the deposition of this compound on any type of substrates at the low temperatures called for in this situation. In addition, there has also been no published research on the deposition of SiC on polyimide composites in particular.

Given the requirements of the product and the constraints on hand, Chemical Vapor Deposition (CVD) is a favored method for deposition of ceramics on polyimides. The primary advantages lie in the flexibility of the technique as well as the large varieties of ceramics that can be synthesized with small variations in the experimental setup. This type of deposition provides for a smooth coverage of rough and irregular substrate surfaces.

In this study, a technique known as plasma enhanced CVD (PECVD) is used, since the deposition of SiC using conventional CVD techniques at temperatures lower than 700 - 800°C is considered impossible. The plasma generated in the reactor provides the additional activation energy to the precursor molecules to decompose to form SiC.

Subsequent to deposition, a number of characterization tests have been carried out to evaluate the properties of the deposited film, such as thickness, adhesion strength, composition and the extent of weight loss inhibition of the coated polyimide. The effect of changing key parameters in the setup, such as substrate temperature, power of the radio frequency plasma, and flow rate of the precursor system into the reactor has also been

studied. Finally, a comparison of weight loss inhibition characteristics afforded by SiC is compared to those obtained from other ceramic coatings such as Al_2O_3 , SiN and SiO_2 .

2.0 Literature Review

Generally, low pressure chemical vapor deposition (LPCVD) of SiC has been carried out in the range of 750 - 1600°C on Si substrates to form satisfactory coatings. At temperatures greater than 1100°C, the deposited films are generally crystalline, while they are amorphous at lower temperatures. Conventional CVD methods are unable to produce satisfactory coatings at temperatures lower than 700°C. It is therefore necessary to provide the system with some source of energy which will lower the reaction temperature; this being essential for deposition on polyimides. In this context, carrying out the reaction in a plasma state serves this purpose by splitting the reactants into positive and negative ions and neutral particles, thus creating conditions more favorable for the individual constituents to dissociate or react. The density of the positive species is equal to that of the negative ones. Of the many possible routes to generate a plasma atmosphere, some commonly used methods use radio-frequency currents or microwaves. SiC has also been deposited by using electron cyclotron resonance PECVD, a method again involving the creation of a type of microwave plasma.

Another important factor to be considered is the Coefficient of Thermal Expansion (CTE) of the polyimide or silicon substrate and the SiC film. If they differ widely, adhesion would be poor due to the varying shrinkage of the two layers upon cooling from the deposition temperature to room temperature. However, it has been found (Satou, et al [1990]) that the range of CTE values for polyimides, from 3×10^{-6} to $15 \times 10^{-6} \text{ K}^{-1}$, is

in the same range as those of silicon and amorphous silicon compounds like silicon nitride, silicon carbide and so on. This would indicate that SiC films either on silicon or on polyimide substrates would not easily peel off due to stresses built up on account of unequal CTEs.

2.1 Deposition of protective films on polyimide composites

There is very little literature available in the area of protective coating of polyimide composites by CVD thin films except for the work done by members of the Materials Research group at Ohio University. Although significant research is said to have been carried out by NASA and by and for the US Air Force, most of the results of this effort have been kept proprietary by the latter. An excellent overview of the topic is given by Harding [1991]. The considerations involved in the use of polyimide composite materials as structural materials are presented as well as a comparison of Chemical Vapor Deposition (CVD) and Physical Vapor Deposition (PVD) as techniques available for laying down thin film coatings on polyimide composites. Finally, the improvement in weight retention as well as the adhesion and morphology of the protective coatings in each instance is evaluated. This paper will be reviewed in detail in this section (2.1).

It was found that amongst a wide range of metal alloys that were deposited on PMR-15 - polyimide based polymer matrix composites (PMC) using dc planar magnetron sputtering (a typical PVD technique), Al and AuPd films displayed the best adhesion

coupled with a reasonable deposition rate. However, the protection from oxidation provided by almost all of the materials deposited was extremely minimal. This may have been due to the intrinsic limitation of sputtering and other PVD methods in terms of limited throwing distance. Since PVD is a line-of-sight procedure, its use for deposition on irregular-surface substrates often yields a non-uniform film.

Two approaches were utilized in the CVD approach: the first using metal organic chemical vapor deposition (MOCVD) with an inorganic precursor (aluminum isopropoxide) and the second using PECVD to deposit diamond-like coatings. The oxidative resistance and adhesion were observed to be significantly better than that provided by coatings made by the PVD approach. Furthermore, the use of a polymeric or metallic compliant layer between the polymer material and the coating was seen to improve both these properties. With regard to processing conditions, it was noted that small carrier gas flow rates (<200 sccm) and high precursor concentrations yielded powdery and fragile films with poor adhesion. On the other hand, low precursor concentrations and high gas flow rates resulted in slow growth rates and continuously amorphous films with good uniformity and adhesion. On prolonged exposure to an oxidative environment, it was observed that the weight retention value of the coating depended more upon the nature of the stress-relieving compliant layer used and the quality of the deposited film (as a result of the processing conditions used) than upon its thickness. Coatings that withstood the thermal stresses imposed at the film-substrate interface during the cool-down period after deposition and did not buckle reduced the

weight loss by as much as 500 percent when exposed to air at high temperatures. However, when the coating integrity was suspect, spalling occurred and the protection provided was minimal. It was also observed that even thick coatings resisted spalling when exposed to prolonged heat treatment in the presence of a compliant layer.

2.2 Low temperature PECVD of SiC

In order to prepare SiC films at lower temperatures in situations where the substrate in question cannot withstand high temperatures, many researchers have used plasma enhanced techniques, using both r.f. and microwave plasma. The precursor systems used in general belong to the silane family with argon and/or hydrocarbons used as the carrier gas.

Delplancke, et al [1991] produced amorphous SiC films using monomethylsilane at temperatures as low as 333 K. They used a 13.56 MHz r.f. generator at 50 W power with resistive heating of the Si substrate over the 333 K - 723 K range. The r.f. electrodes consisted of two horizontal stainless steel rods separated by a gap of 2 cm. The deposition occurred on the lower electrode which was heated. The plasma chamber was connected through a differentially pumped middle stage to a mass analyzer to carry out mass spectroscopy. Before deposition, the silicon wafers were etched for 5 minutes in 49% hydrofluoric acid to remove the oxide layer. Gold foils were prepared for deposition by polishing with a paste of alumina and rinsing with acetone and methanol.

Profilometry was used to measure film thickness and X-ray diffraction (XRD) was carried out to examine its crystal structure. Auger electron spectrometry (AES) and X-ray photoelectron spectrometry (XPS) characterization of the films was carried out to evaluate the surface composition; argon depth profiling was carried out over 1 cm² area for XPS and a 1mm² area for AES with ion energies of 3 and 5 keV respectively. The following conclusions were reached:

- ▶ XRD analysis showed that the films possessed an amorphous structure over the entire range of temperatures.
- ▶ Mass spectroscopy studies of the CH₃SiH₃ plasma indicated that no species with over 46 a.m.u. was present in the plasma, indicating low polymerization in the gas phase. The gas phase predominantly contained species with unbroken Si-C bonds; on comparison with a SiH₄ - CH₄ precursor system, the latter showed the presence of fewer SiC bonded species. It was also observed that temperature did not affect the spectra obtained.
- ▶ The deposition rate was found to decrease with an increase in substrate temperature. This was explained by the increasing self bias on the lower electrode due to the process of resistive heating, with a self-bias of 275 volts being measured at 773K. This would reduce the movement of the positive species containing the Si-C bonded units towards the substrate electrode.

- ▶ AES and XPS revealed that there were two phases present, an SiC rich phase and an amorphous carbon phase due to the presence of both binding energies for the 1s carbon in the respective spectra. It was observed that the SiC was not stoichiometric in the SiC phase, and instead richer in Si. In addition, the films deposited on the powered electrode, while less thick, showed a higher presence of Si than those deposited on the lower electrode. These films also contained a lower percentage of oxygen contamination.
- ▶ Oxygen contamination of the films was observed at lower temperatures (as high as 15 %), but was significantly reduced for substrate temperatures above 423 K.

Bielan and Arendt [1992] reported the deposition of high quality SiC layers on 100 mm diameter silicon wafers using precursors of the form R_3SiX , where $R=CH_3$, C_2H_5 , C_4H_9 , and $X=H$, Cl , CH_3 , R_3Si , and so on. The intention was to use a single liquid precursor with a carrier gas instead of the gaseous silane-hydrocarbon precursor systems commonly used for obtaining SiC thin films. This is desirable since such systems are extremely explosive and SiH_4 is also a highly toxic compound.

The deposited coatings were free of cracks and showed good adhesion to the substrate. The deposition was carried out in a 13.56 MHz r.f. plasma at a pressure range of 13 to 68 Pa. They achieved a thickness uniformity that varied between 0.5 % to 2 %

over a 100 mm² surface. Their films also displayed excellent temperature stability up to 900°C, with no variation in the Si:C ratio and no detachment of the film from the substrate. XRD studies showed that the film was amorphous in nature.

In order to evaluate the composition of the deposited layer, AES was employed; a variation of the r.f. power and gas pressure was accompanied by a corresponding variation of the percentage of carbon from 40% to 68%. In comparison, the Si content varied from 32% to 45%. It was also observed that the formation of SiC is extraordinarily sensitive to the presence of oxygen in the sample. For carbon contents of over 60% and $x > 0.45$, where

$$x = \frac{[Si]}{[Si] + [C]}$$

it was observed that the extent of oxygen contamination was less than 2% whereas for low carbon content (~50% C, $x < 0.4$), the oxygen concentration was as high as 17%.

Yasui, et al [1992] have reported a slightly different method of PECVD for a tetramethylsilane precursor system. They used hydrogen radicals to extract the hydrogen from the methyl groups to ensure the formation of a homogeneous SiC film in stoichiometric ratios, with low hydrogen concentrations in the deposited coatings. They seemed to have been successful in limiting the formation of Si_{1-x}C_xH that is common under the conditions that the reactions occur, namely, low temperatures and pressures in plasma environments with precursor species rich in hydrogen. They used microwaves at

2.45 GHz with a power of 120 - 140 W at a pressure of 266 Pa. While they did not measure or control the substrate temperature, they estimated it to be in the region of 250 - 300°C. FTIR studies were performed to study the composition and structure of the deposited film.

2.3 Tetraethylsilane (TES) as a precursor for SiC

A vast majority of the work done in CVD studies of SiC involves the use of silane-based compounds as a precursor with hydrogen and/or hydrocarbons as carrier gases. In general, thin SiC films have been successfully deposited using systems of the form $\text{Si R}_{4-n}\text{X}_n$ (where R corresponds to H, CH_3 , C_2H_5 , and so on, and X to Cl or H, with $0 \leq n \leq 4$) with hydrogen and/or C_2H_2 as carrier gases. The two drawbacks with these systems are:

1. The presence of Cl or any other halide leads to a highly corrosive atmosphere during deposition that leads to high costs in terms of equipment protection and replacement.
2. Stringent safety precautions have to be taken owing to the pyrophoric and inflammable nature of the highly reactive precursor mix.

Maury, et al [1989] have investigated the use of a single liquid precursor that would deposit satisfactory films of SiC without all of the above hazards. Given the knowledge that tetramethylsilane (TMS) had been successfully used for LPCVD SiC

deposition, they have attempted to use TES, since it is easier to split ethyl radicals than their more stable methyl counterparts. They have obtained satisfactory amorphous coatings of $\text{Si}_x\text{C}_{1-x}$ on Si, Al_2O_3 and SiO_2 substrates at 800 - 1000°C and 10 Torr which show good morphology and optical properties. The Vickers microhardness was measured to be 1.81, which corresponds to that cited in literature for CVD SiC. EDX and IR spectroscopy also confirmed the presence of SiC in the deposited films. To verify the role of hydrogen as a carrier gas, they have studied these properties by substituting helium and have found no significant differences, indicating that an inert carrier gas conveying TES precursor can produce satisfactory coatings without the necessity of potentially hazardous hydrogen.

3.0 Experimental Setup and Procedure

3.1 Process considerations

As mentioned earlier, the choice of a deposition process is limited by the temperature that the polyimide composite substrates can withstand without degrading. Also, silicon carbide cannot easily be sputtered or deposited by any physical deposition process. This dictates the need for a CVD process at low temperature. However, SiC has rarely been deposited at temperatures below 700°C by conventional CVD methods; hence the need for a plasma enhanced CVD (PECVD) process.

3.2 Precursor considerations

In most earlier studies of SiC formation by CVD, silanes and their alkyl and halo-derivatives have been successfully used. However, the more the substitution of SiH₄, the safer the substituted compound in terms of air and moisture sensitivity, pyrophoric, and corrosive behavior (Kwatera [1990]). Therefore, tetraethylsilane, Si(C₂H₅)₄, was chosen as a single precursor, the source for both the Si and the C. It is a colorless, volatile liquid at room temperature with a vapor pressure of 760 torr at 153°C and a pressure of 200 torr at 108°C (Bielan and Arendt [1992]). Argon was used as the carrier gas and was bubbled through the SiEt₄, which is maintained at room temperature. The gas was passed through

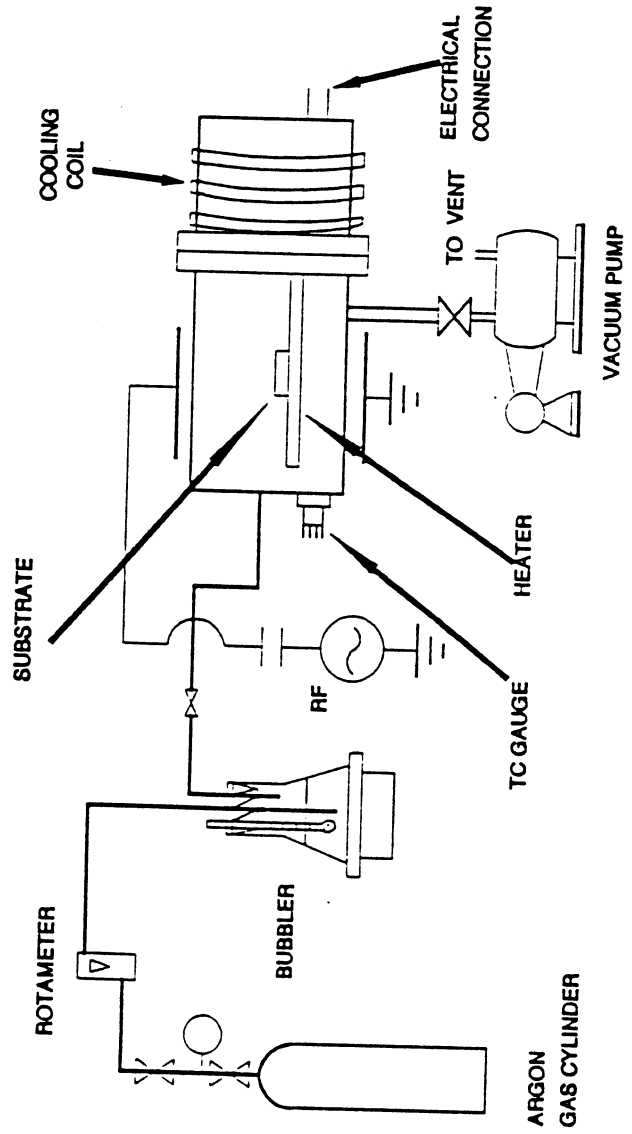
a rotameter to measure flow rate and then passed into the reaction chamber through 1/4 inch diameter stainless steel tubing.

3.3 Reactor considerations

The reaction chamber was evacuated by means of a mechanical pump to about 13.3 Pa, and the plasma was generated by 13.56 MHz r.f.waves, with the power being varied between 0-150 W. The substrate was placed on a flat heater plate along the direction of the gas flow, and its temperature measured by a thermocouple in contact with the heater used to maintain the substrate temperature at the required value. The heater was 5.08 cm wide and 10.16 cm long. The thermocouple reading was compared with actual measurements of the temperature on the substrate surface using an independent digital thermocouple thermometer and a calibration is made based upon the temperature readout corresponding to the potentiometer reading. This was necessary since the readout obtained from the thermocouple on the heater surface is skewed once the reactor has a plasma generated within.

Since deposition on the substrate alone is of interest, cold water was passed through coils on the outside of the copper walls in order to keep them cool (Cold Wall PECVD) and prevent any reaction thereon. Figure 1 shows the setup. The reactor as a whole was patterned after a design by NASA and the external brass chamber (including

FIGURE 1. EXPERIMENTAL SETUP



COOLING COIL

ELECTRICAL CONNECTION

TO VENT

VACUUM PUMP

HEATER

TC GAUGE

SUBSTRATE

RF

BUBBLER

ROTAMETER

ARGON GAS CYLINDER

a heater plate and external cooling water coils) was fabricated at Ohio University. The diameter of the 15.24 cm long cylindrical glass tube in which the plasma is generated is 11.43 cm. The precursor enters through a 0.5 cm diameter tube within this chamber which has pinholes equally distributed along its length in order to distribute the reactant throughout the plasma. The glass reactor also has an outlet to the vacuum pump as well as a port to which a pressure gauge is connected. The brass chamber has ports to connect the power supply to the heater as well as to the thermocouple thermometer.

3.4 Substrate considerations

The substrates used were graphite-fiber polyimide composites supplied by NASA and commercially available silicon wafer substrates. The need to use silicon substrates is due to the difficulty in measuring the film thickness and adhesion strength of the film on polyimide composite substrates, which are highly irregular on the surface. During deposition, silicon substrates are "shielded" by using a smaller piece of silicon to cover a part of the original substrate, so that the profilometer can measure the step increase in height between the shielded and exposed portion of the substrate in order to give the thickness of the film. It is also important to ensure that the position of the substrate on the heater plate is unchanged through all the runs, so that its position in the reactor does not become a variable in the deposition process. This is due to the fact that temperatures along the heater plate were found to vary by 20 - 30°C depending upon the distance of

the point of measurement from the welded joint between the heater base and the brass chamber.

3.5 Post-deposition analysis

Following deposition, the following experiments were carried out:

1. Thickness measurement using the profilometer.
2. Adhesion strength testing.
3. Weight loss measurements at sustained high temperatures in an oven.
4. XPS and Auger electron spectroscopy to detect the presence of SiC bonds and the composition of the thin film.

Appendix II contains a list of the equipment used and their specifications.

3.5.1 Profilometry

This method of thickness measurement involves the analysis of the vertical movement of a diamond stylus as it traces a path along the film surface. The film thickness is directly read out as a magnification of the step contour movement along the surface topography. The downward stylus force is maintained at a constant 25 mg. Powdery or soft films may not be analyzed by this method as the stylus penetrates into the film bulk. Rough or unclean surfaces may introduce extraneous noise and must be avoided. Due to the sensitivity of the 10 μm stylus, a stable mounting of the apparatus

is essential. Profilometry is a markedly better method than the older procedure to measure thickness based on the weight of the film and an assumption of a uniform density, using the following expression :

$$d = \frac{m}{A \rho}$$

where d is the thickness, m the mass, A the area under consideration and ρ the bulk density of the film. This assumption of a uniform density is often not true due to the presence of voids and non-uniform deposition.

3.5.2 Adhesion strength measurement

The adhesive property is quantified by the force required to remove a small area of the film from the substrate on which it is coated. To this end, the adhesion tester provides a measured force to a stud that is attached to the surface by an epoxy glue while the substrate is held motionless. It works on the assumption that the force applied is completely utilized by the small area in question, and not contributing to any deformation of the entire film surface. Thus, it is important that the total film area on the sample is large in comparison to the area on which the force is applied. It is also necessary to note the difference between the force that may register as a result of the substrate failure and that which removes the film leaving the substrate intact and undeformed. Due to the

nature of the stud-film interfacial bond, it is necessary that the film be smooth; this precludes the adhesion strength measurement of films on irregular surfaces.

3.5.3 Weight loss analysis of polyimide composites

The ultimate goal of the coatings of ceramic materials on polyimide composites is to evaluate their effectiveness in protecting the polyimide from thermo-oxidative degradation. An indicator of this degradation phenomenon is the extent of weight loss at elevated temperatures in the presence of oxygen due to the liberation of the oxides of carbon, hydrogen and nitrogen. A comparison between the percentage loss of uncoated and coated samples yields information on the improvement offered by the coating.

3.5.4 Electron spectroscopy

Electron spectroscopy is the basis for both AES and XPS techniques; when a beam of electrons is incident upon an atom, it can cause an electron from an inner atomic shell to be excited and leave its shell, thus creating a hole or vacancy in that shell. In the filling of this vacancy, an electron from an outer shell expends this energy by in turn expelling an electron from yet a third level. A measure of the energy of this expelled electron (the Auger electron) is indicative of the chemical state of the atom, and is the basis for AES. In the case of XPS, instead of an excitation source of electrons, low energy X-ray photons cause electrons to be expelled out of the atom by the photoelectric

effect. Given that the photoelectron energy is unique for an element in a given chemical state, this phenomena provides for the identification of the elements present in the sample. Since the quantity to be measured in both cases is the energy of electrons expelled from the surface of the sample being analyzed, they are often included in tandem in the same apparatus. Typically, the ability to etch surfaces in order to analyze successive layers of the sample is also included in such equipment, since both AES and XPS are surface sensitive techniques and cannot penetrate beyond a few monolayers from the surface. In both types of spectroscopy, the analyzer potential is set so that electrons of a given energy alone enter it; the number of such electrons versus the energy at which they are collected is the basis for XPS and AES plots. Since the number of Auger electrons is very small compared to the total number of electrons being expelled, it is magnified by a numerical or electronic differentiation of the electron count with respect to the energy at which they are collected.

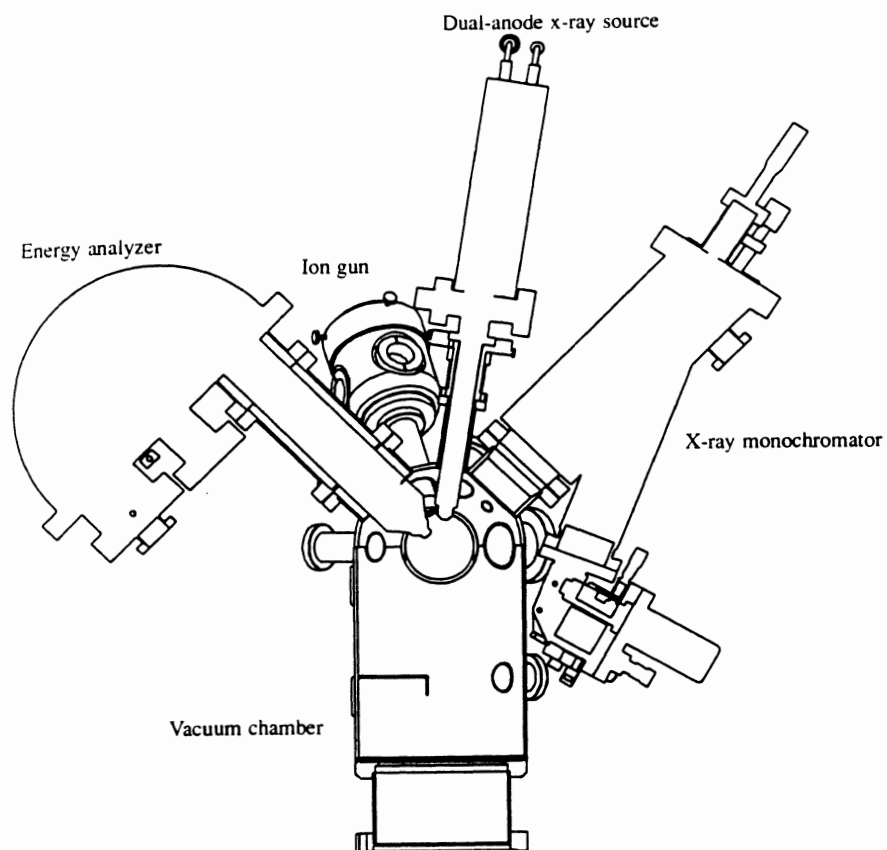


Figure 2 : A typical AES/XPS experimental setup

3.6 Procedures

3.6.1 SiC Deposition

1. The silicon substrate is cleaned with acetone and placed on the substrate heater. Care must be taken to avoid the presence of dust or fingerprints on the silicon or polyimide substrate.
2. The vacuum pump is turned on and the pressure measured to ensure that the pressure does not exceed 0.1 torr. In the event that it does, the system must be checked for leaks.
3. The heater plate in the reaction chamber is raised to the desired temperature and cooling water is introduced through the external coils of the brass chamber.
4. The r.f. plasma generator is switched on; care must be taken to ensure that the pressure is not above 0.1 torr, since a high pressure in the chamber with the plasma on could burn out the reactor. A low start-up plasma power is advisable before the introduction of argon into the system.
5. Argon is introduced into the chamber through a bypass valve for two minutes.
6. The bypass valve is closed and the argon is bubbled through the TES precursor at the required flow rate. Care must be taken to ensure the same gauge pressure in the argon tank for all runs.

7. The plasma must now be tuned in order to ensure the maximum power throughput. This is done using the variable capacitive impedance in the reactor. The reactor is designed to set off an alarm if impedance matching has not been achieved. Failure to tune the system may result in the burnout of the plasma generator.
8. The r.f. plasma power is set to the required level and the power, argon flow rate and substrate heater temperature are monitored manually throughout the duration of the run.
9. After the desired deposition time has, the r.f. generator, substrate heater and precursor hot plate are switched off. The argon is again rerouted through the bypass valve in order to carry any by-products of the reaction out of the system.
10. When the substrate heater temperature falls below 75 °C, the argon line is closed and after 5 minutes, the chamber is vented. The samples are removed and placed in boxes while ensuring that the surface is not contaminated by fingerprints or dust.

3.6.2 Film Thickness and Uniformity

1. The Dektak IIA profilometer is turned on and the sample conveyed to the platform. The camera is focussed onto the region of examination and the platform levelled by running a test run and using levelling knobs to raise or lower the platform as the diamond stylus runs across the sample.

2. Program specifications for the test are input. These consist primarily of the length of the run of the diamond stylus, its speed and data levelling criteria.
3. The test is started; the reference cursors on the profilometer screen are moved along the graph obtained to fix the point at which a step increase in height is obtained. The value of the height at this point is then read. If necessary, the part of the run along the shielded portion of the sample is levelled to obtain the true height of the film. The result of each run may visually be read off the screen or the entire graph may be printed out. The data points along the path of the stylus may also be stored in a PC.
4. It is necessary to calibrate the profilometer periodically; this involves checking the height read off by the program with standard step increase samples as well as the evaluation of the downward force of the stylus on the sample surface, which should be within manufacturer specified limits.

3.6.3 Film adhesion strength

1. Samples must be prepared by the attachment of epoxy coated studs on to the film surface before adhesion tests can be carried out. This is done by placing the samples on special holders and introducing epoxy coated studs on the film surface. These studs must be kept in a refrigerated environment, failing which the epoxy will degrade.

2. The entire assembly is then placed in an oven at 150 °C for 90 minutes to allow the epoxy to cure and form a firm bond between the stud and the film surface.
3. The assembly is then allowed to cool to ambient temperature and the special holders removed. The sample with the stud is then placed in the jaws of the Sebastian Five-A adhesion tester.
4. An IBM PC compatible with the Zeta34 software that accompanies the adhesion tester is switched on and the software is executed. The video camera and monitor are also switched on.
5. The tester jaws are tightened, ensuring that the sample is parallel to the floor and the stud is perpendicular to the machine with 0.25 inches left outside the jaws. The downward speed of the jaws and the force applied are adjusted according to the accuracy required.
6. The run is started; data is recorded on the PC and the path of the sample downwards is monitored on the monitor screen. The point at which the stud breaks free of the sample is noted and the experiment terminated. Care must be taken to keep a distance from the sample and to wear protective glasses, as the sample may shatter, throwing pieces in all directions.

3.6.4 Weight loss experiments

1. Coated and uncoated polyimide composite samples are weighed in a high accuracy electronic balance.
2. An oven is heated to 375 °C and 15 minutes are allowed to elapse before introducing coated and uncoated polyimide composite samples.
3. Samples are removed at desired intervals and weighed. Care must be taken to ensure that the weighing balance is periodically calibrated. It must also be ensured that the upper surface of the sample that is exposed in the oven is the surface that has been coated by SiC.

3.6.5 Compositional Analysis - XPS/AES experiments

In order to evaluate the compositional breakdown of the deposited film, X-ray photoelectron spectroscopy (XPS) and Auger electron spectroscopy (AES) have been carried out at the Edwards Accelerator Laboratory in Ohio University.

1. The coated sample is cut to a size of approximately 2 cm x 2 cm using a diamond cutter and mounted on a sample holder. A silver based adhesive is applied to the sample base and is allowed to cure.
2. The sample holder with coated wafers is loaded on to a carousel that can hold 10 samples at one time, and the carousel assembly is introduced into the evacuated analysis chamber.
3. A V-shaped prong lifts the sample holder from the carousel into the analysis position and the position coordinates are noted.

4. Object specifications for the run are set on the Sun Sparc Workstation linked to the reactor and the excitation source electronics. The excitation source (Al or Mg X-rays for XPS or a 2 keV electron beam for AES) is tuned in order to minimize the signal to noise ratio in the spectra.
5. An initial sweep of the entire range of binding energies (for XPS) or kinetic energies (for AES) is carried out in order to roughly identify the species present. This may be done using a built in library available with the system.
6. Having identified the predominant species, narrow bands of binding or kinetic energies are specified for better resolution. The number of runs to be taken in order to produce the final spectra is specified. The XSAM system averages out the counts from the specified number of runs in order to obtain data for the output plot.
7. Once the run is completed, the plot may be viewed and quantification carried out by the XSAM software. Again, shifts in energy, if any, from the elemental energy states may be analyzed using the in-built library. Specific peaks may be tagged at this point.

3.7 Safety considerations

The Material Safety Data Sheet (MSDS) for tetraethylsilane is appended as Appendix I. Safety precautions are taken as suggested, with reference to handling and

protective clothing. First-aid and fire-fighting equipment as required by the MSDS are present in the laboratory. As argon is the carrier gas, the problem of hazardous combustion or decomposition is avoided. Also, since the precursor in the inlet stream is in very dilute concentrations to the reaction chamber, the amount of unreacted TES being carried through to the exhaust by the vacuum system is negligible. The compound is not pyrophoric, and care is taken to ensure that there are no sparks and open flames present in the environment.

Safety goggles must be worn during the adhesion testing experiments as the sample often shatters with pieces being dispersed in all directions. Care must also be taken during XPS experiments to avoid looking at the sample while the X-ray gun is being fired; aluminum foil shields must be placed over all open ports of the analysis chamber.

4.0 Results and Discussion

Table I shows a summary of the experimental conditions and the data collected from the deposited samples through profilometry and adhesion testing.

4.1 Thickness measurement

The thickness of the deposited film measured by profilometry divided by the deposition time yields the deposition rate whose variation with temperature, flow rate and r.f. power is analyzed. The accuracy of the equipment used for profilometry is around 97%. The procedure to be followed is mentioned in the Chapter 3.

4.1.1 Deposition rate versus temperature

It is observed that the deposition rate increases steadily with increase in substrate temperature at a given argon flow rate and r.f. power. This is consistent with a kinetic theory type of reaction, whereby an increase in substrate temperature increases the energy available to surmount the activation energy for the decomposition reaction of TES. However, the absence of a levelling of the deposition rate at 300 - 350°C indicates that even higher rates may be obtained if it were possible to increase the substrate temperature. While data is not available for SiC deposition rates at these low

**Table I : PECVD process parameters
and data for silicon samples**

Temperature (deg C)	Flow rate (ml/min)	Power (Watts)	Time (min)	Thickness (Å)	Dep. Rate (Å/min)	Adhesion (MPa)
150	260	100	15	1180	79	SF*
150	260	100	15	1210	81	SF
150	718	100	15	940	63	SF
165	260	100	15	1340	89	48.36
165	489	100	15	1150	77	SF
165	718	100	15	1020	68	50.85
220	718	100	15	1610	107	SF
225	260	100	15	1810	121	SF
230	260	100	15	1870	125	45.07
230	489	100	15	1800	120	SF
230	718	100	15	1640	109	46.39
250	260	100	15	2210	147	SF
250	260	100	15	2140	143	SF
285	260	100	15	2510	167	SF
285	718	100	15	1910	127	SF
290	260	100	30	5040	168	47.69
290	260	100	15	2600	173	43.74
290	489	75	15	-shattered-	- nil -	SF
290	489	75	15	2270	151	SF
290	489	100	15	2460	164	SF
290	489	100	15	2510	167	SF
290	489	125	20	-powder-	- nil -	SF
290	489	125	20	-formation-	- nil -	SF
290	489	125	20	3480	174	39.73
290	489	125	15	2630	175	SF
290	489	125	10	1690	169	SF
290	718	100	15	2000	133	44.30
300	260	100	15	2580	172	SF
325	260	100	15	2780	185	SF
325	718	100	15	2490	166	SF
350	260	100	15	2950	197	SF
350	260	100	15	2990	199	41.90
350	489	75	15	2560	171	SF
350	489	100	15	2890	193	SF
350	489	100	15	2880	192	42.30
350	489	100	30	5850	195	44.11
350	489	125	20	4090	205	41.64
350	489	125	15	3040	203	SF
350	489	125	10	2030	203	SF
350	718	100	15	2680	179	43.03

*SF = Sample failure prior to failure at the coating-substrate interface

temperatures (below 700°C), the data obtained shows a good comparison with rates obtained in the deposition of other ceramic materials at this range of temperatures (Gopal [1991], Neogi [1992] and Miller [1991]). Figures 3, 4 and 5 are plots of deposition rate versus temperature for different argon flow rates.

At lower temperatures, it was noted that the formation of a film was erratic, and powder formation was a common occurrence. This was especially true at low r.f. power and high flow rates and may have been due to the low rates of reaction at the substrate surface due to insufficient activation energy. It is also possible that surface diffusion of the reaction product species was hindered due to the higher concentration of precursor at the substrate surface on account of the high argon flow rate.

4.1.2 Deposition rate versus argon flow rate

Figure 6 displays the variation of the deposition rate with changing argon carrier gas flow rate. It is seen that for the entire range of temperature from 165 to 350°C, the deposition rate decreases with increasing flow rate. While the trend is not exactly mirrored for each of the temperatures, we see in general that there is a 10 - 20 % drop in the rate as the flow increases from 260 ml/min to 718 ml/min.

This may be due to the fact that larger gas flow rates involve a greater TES concentration in the reactor, whereas it has been reported in literature that high deposition

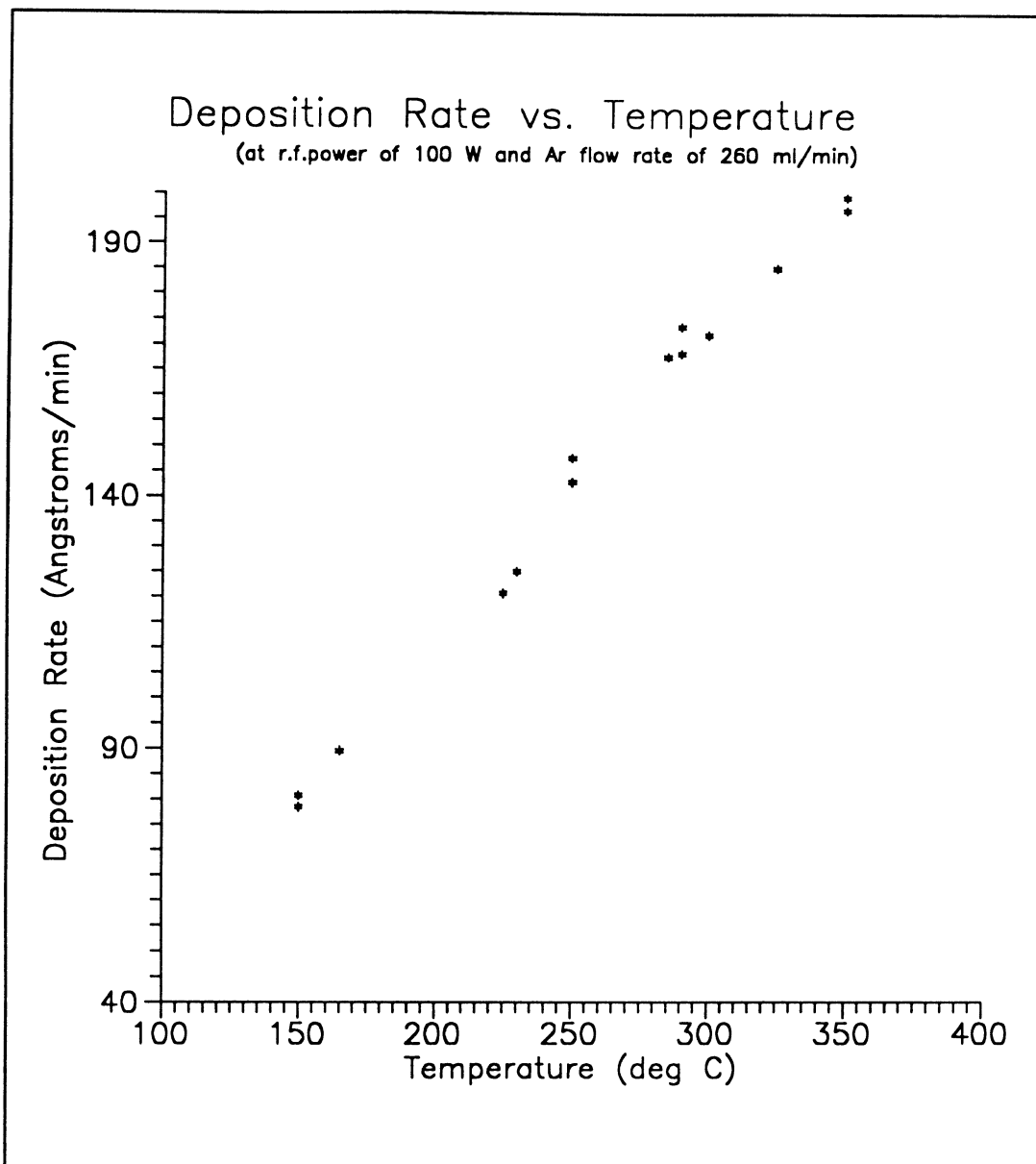


Figure 3 : Deposition rate versus Temperature for argon flow rate of 260 ml/min and r.f. power of 100 W

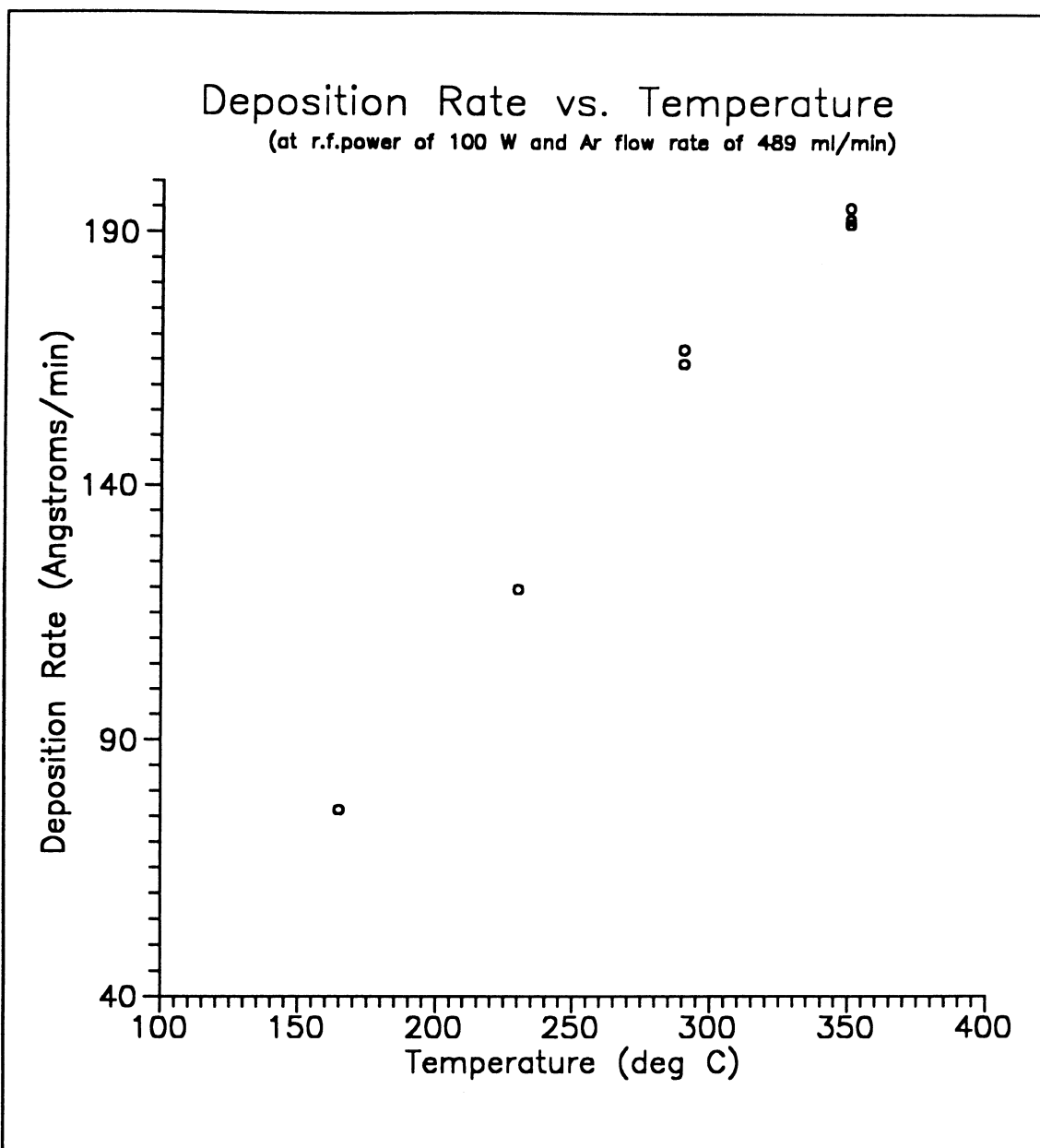


Figure 4 : Deposition rate versus Temperature for argon flow rate of 489 ml/min and r.f. power of 100 W

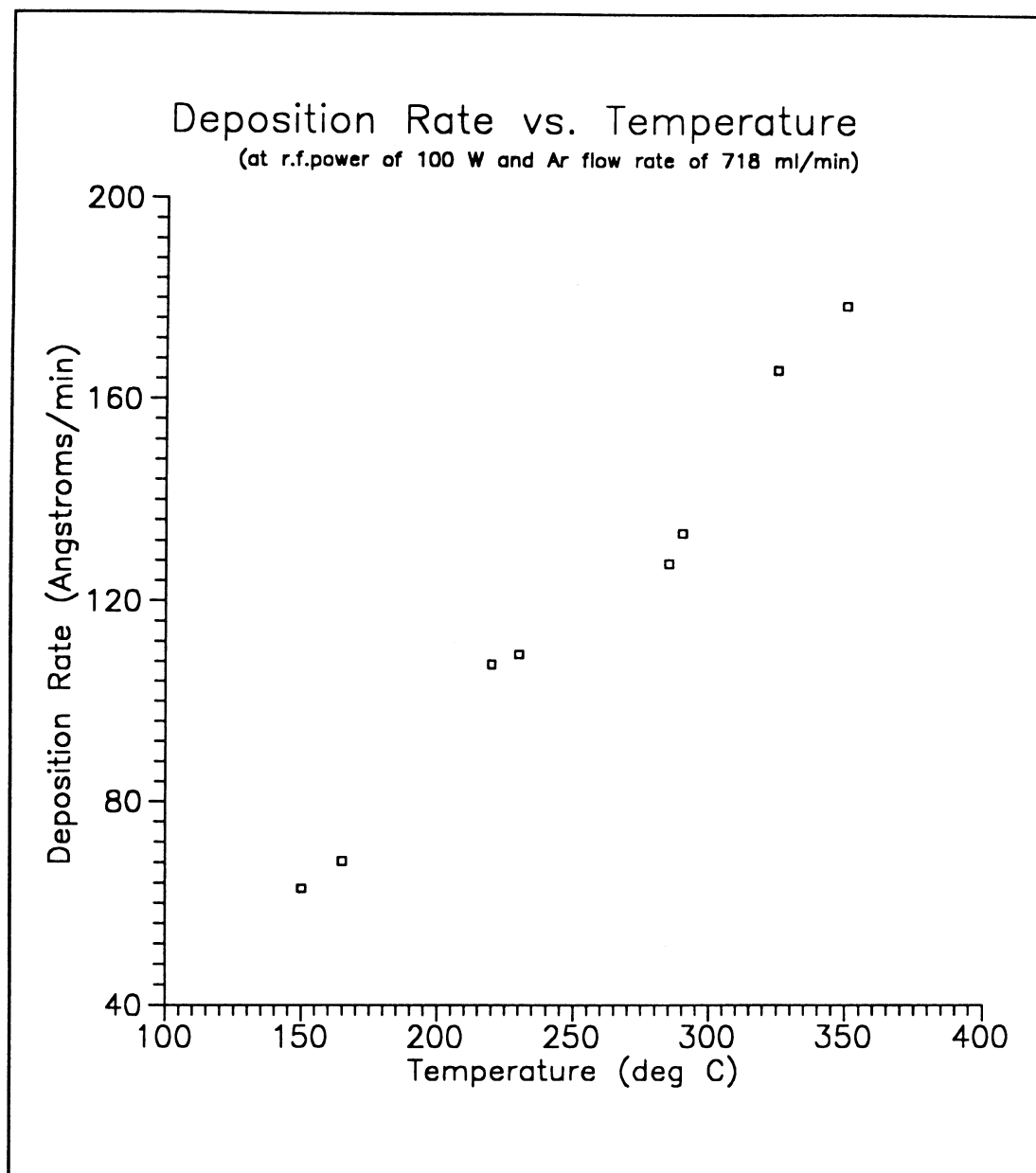


Figure 5 : Deposition rate versus Temperature for argon flow rate of 718 ml/min and r.f. power of 100 W

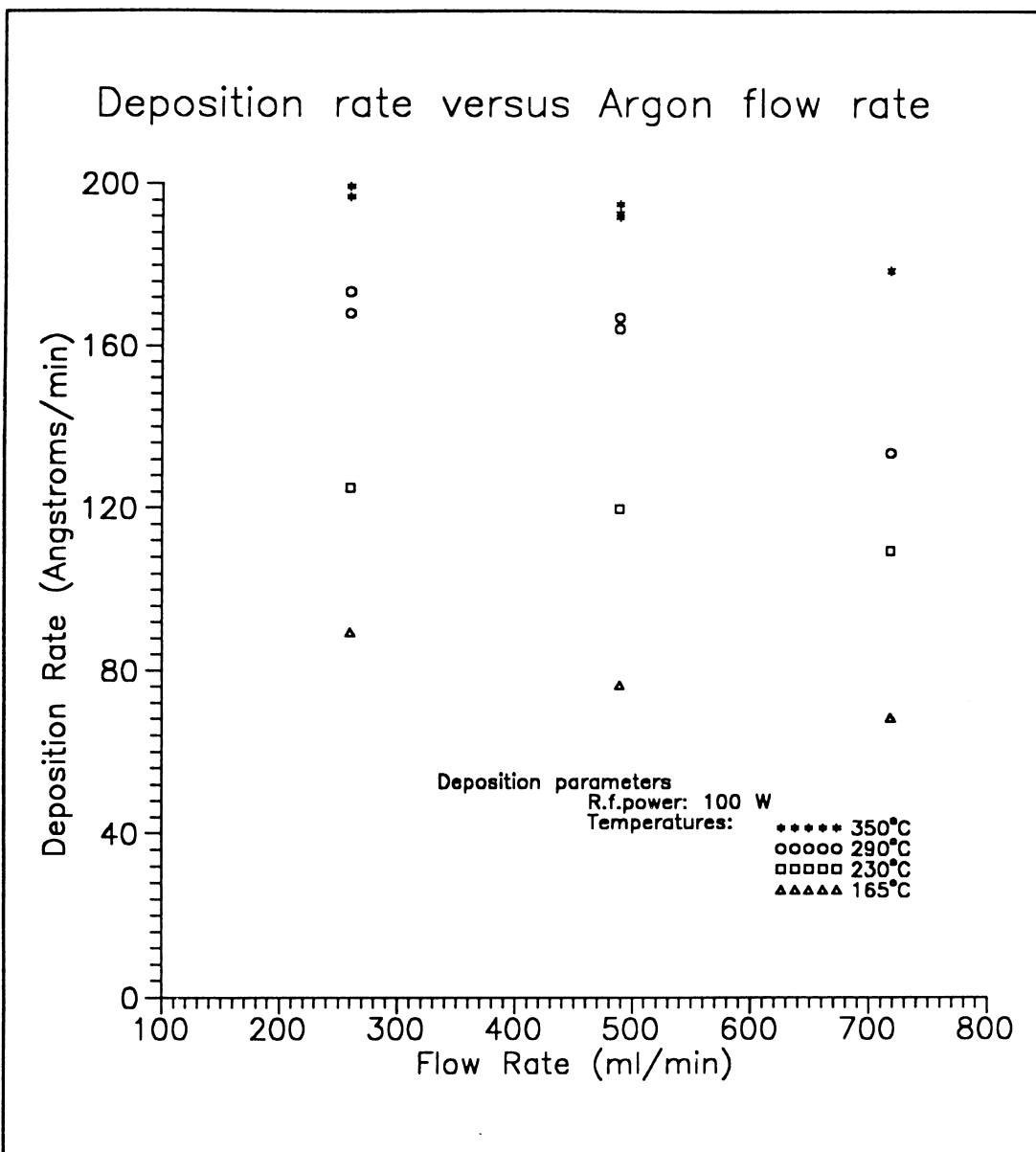


Figure 6 : Deposition rate versus Argon flow rate at an r.f. power of 100 W and temperatures of 165, 230, 290 and 350°C

rates are generally supported by low precursor concentrations and high temperatures (Figueras et al [1991]). Also, with a higher gas flow rate through the reactor, the residence time of TES in the plasma environment over the substrate surface is reduced. In addition, an increase in flow rate results in the elevation of the reactor pressure, which in turn reduces the efficiency of the plasma in breaking up the TES molecule.

However, this contradicts the findings of certain other research of deposition rate dependency on flow rate (Miller [1991]) wherein it has been stated that higher gas phase velocity at the substrate surface results in greater transport and hence a higher deposition rate on the surface.

Another factor which has not been examined in this study, and which may have a bearing upon the influence of the flow rate upon the deposition rate, is the question of the flow pattern of the incoming gas stream as it flows through the reactor and into the outlet. It is possible that at higher flow rates, the pattern is such that the precursor is not satisfactorily reaching the heater plate upon which the substrate is placed.

4.1.3 Deposition rate versus r.f. power

As may be expected, increasing r.f. power has the effect of improving the deposition rate. This is due to the enhanced splitting of TES molecules into reactive ions

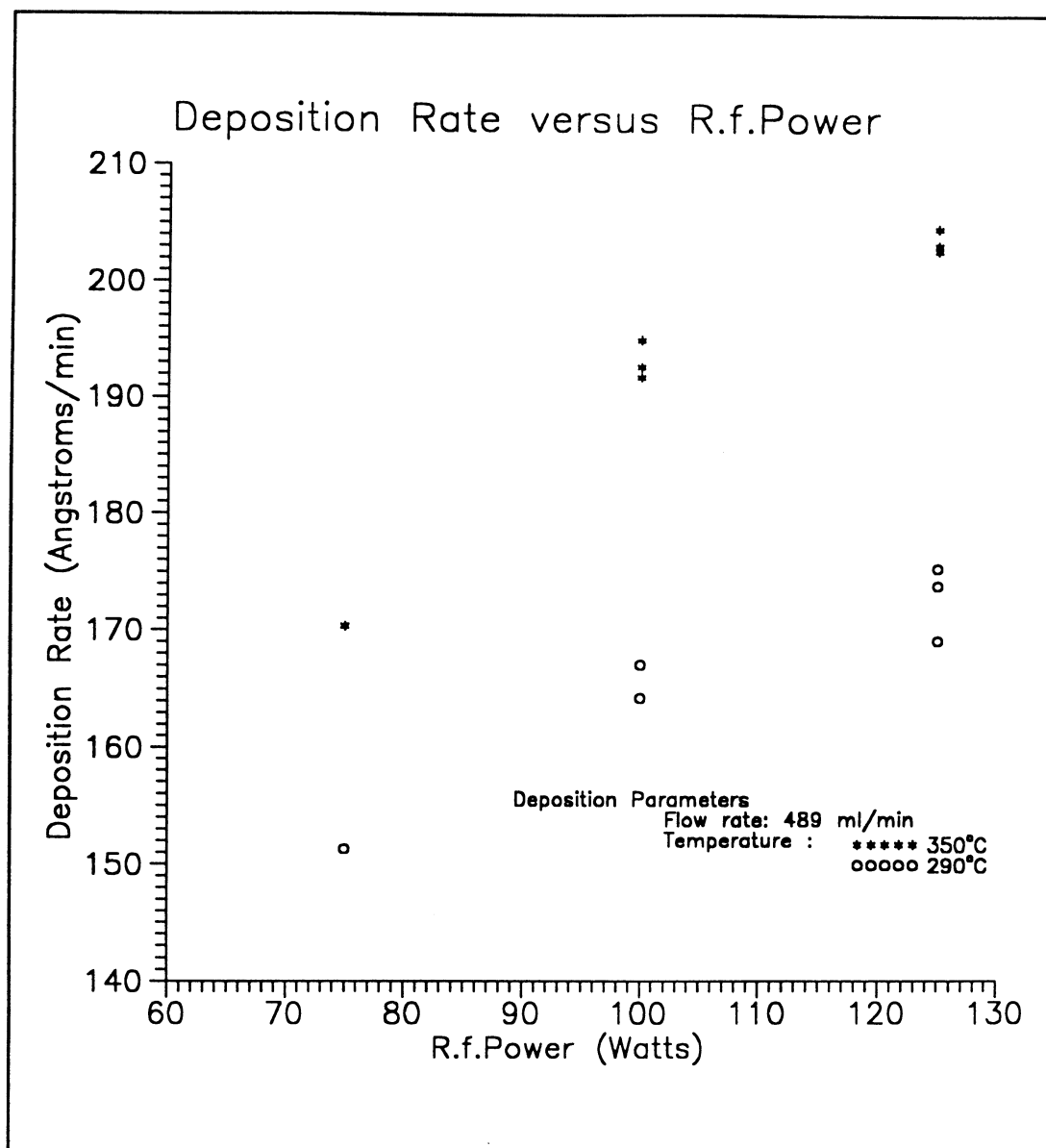


Figure 7 : Deposition rate versus r.f. power at an argon flow rate of 489 ml/min and temperatures of 290 and 350°C

in the gas phase, which in turn reduces the activation energy necessary to be provided by the substrate heater. This may be seen in Figure 7.

However, it is noted that there is a slight levelling off of the increase in deposition rate with increased power. This is probably due to the fact that the ionic species in the plasma are polarized and unable to move freely to react with other species therein, due to the attraction or repulsion from the r.f. field generated by the external plates. Also, depending on their charge, the species are attracted to or repulsed from the center of the reactor, where the substrate heater is located.

Due to the limitations of the deposition equipment, it was difficult to maintain a constant power of 125 W over the 15 - 30 minute duration of each deposition. It was also extremely difficult to maintain a plasma at higher power levels (> 125 W) due to problems with tuning the circuit (operating the equipment with the plasma not tuned is deleterious to the coils powering the setup).

4.1.4 Thickness uniformity

The following expression is used to compute thickness uniformity:

$$\% \text{ variation} = \frac{100 * (D_{\max} - D_{\min})}{(D_{\max} + D_{\min})}$$

where D is the film thickness and D_{\min} and D_{\max} are the minimum and maximum observed thicknesses in the area of examination.

In general, the deviation in thickness of the deposited films was within 5 % over a small surface of 7.5 mm x 7.5 mm. However, over larger areas, this uniformity deteriorates rapidly. Table II displays the measurements over a 1.5 cm x 1.5 cm area, showing variations of over 10 %, especially for films deposited at lower temperatures. Possibly, the unequal heating of different parts of the substrate surface at lower temperatures may have contributed to so called "cold spots", where the surface reaction has proceeded slower than neighboring regions.

It may be noted that the non-uniformity appears to increase with a decrease of film thickness. In light of the limitation in accuracy of the profilometer, it is also possible that for thinner films, this variation in accuracy as a percentage deviation becomes more pronounced. Another noteworthy observation is that the absolute difference in thickness (shown in Table II) is nearly constant for all the samples. This may indicate that the variation of the thickness uniformity is more due to measurement error than actual deposition characteristics.

Table II : Thickness Uniformity over 2.25 sq. cm

Temperature (deg C)	350	290	350	290	290	230	150
Flow rate (ml/min)	489	260	489	489	260	718	718
Power (Watts)	100	100	125	125	100	100	100
Thickness	5850	5040	4090	3480	2600	1640	940
Thickness: Max	6210	5390	4480	3910	3070	1980	1190
Min	5760	4910	3920	3320	2510	1550	890
% Variation	3.76	4.66	6.67	8.16	10.04	12.18	14.42

4.2 Adhesion measurements

Adhesion strength measurements were carried out using a Sebastian Five-A tester according to the protocol mentioned in the previous chapter. The data was obtained from the analysis run by Zeta (Version 3.4) software run on an IBM PC compatible computer linked to the tester.

The phenomenon of variation in adhesion strength vis-a-vis independent variables such as temperature and flow rate is not clearly understood. Conflicting reports have been made in literature regarding its trend (or absence thereof) in instances of ceramic thin films like titanium nitride and aluminum oxide on silicon (Mattox [1988], Lorenz [1988], Miller [1991], Neogi [1992]).

4.2.1 Adhesion strength versus temperature

In this study it was found that there is a decreasing trend in adhesion strength with an increase in substrate temperature as seen in Figure 8. This may be due to the increased thermal stresses involved due to the difference in the coefficient of thermal expansion between the film and the substrate. In addition, it is possible that in films that have been deposited at higher deposition rates, residual film growth stresses are higher. It was not possible to measure the stress on the substrate due to the small size of the samples; the stress gauge requires standard 2 inch diameter silicon substrates.

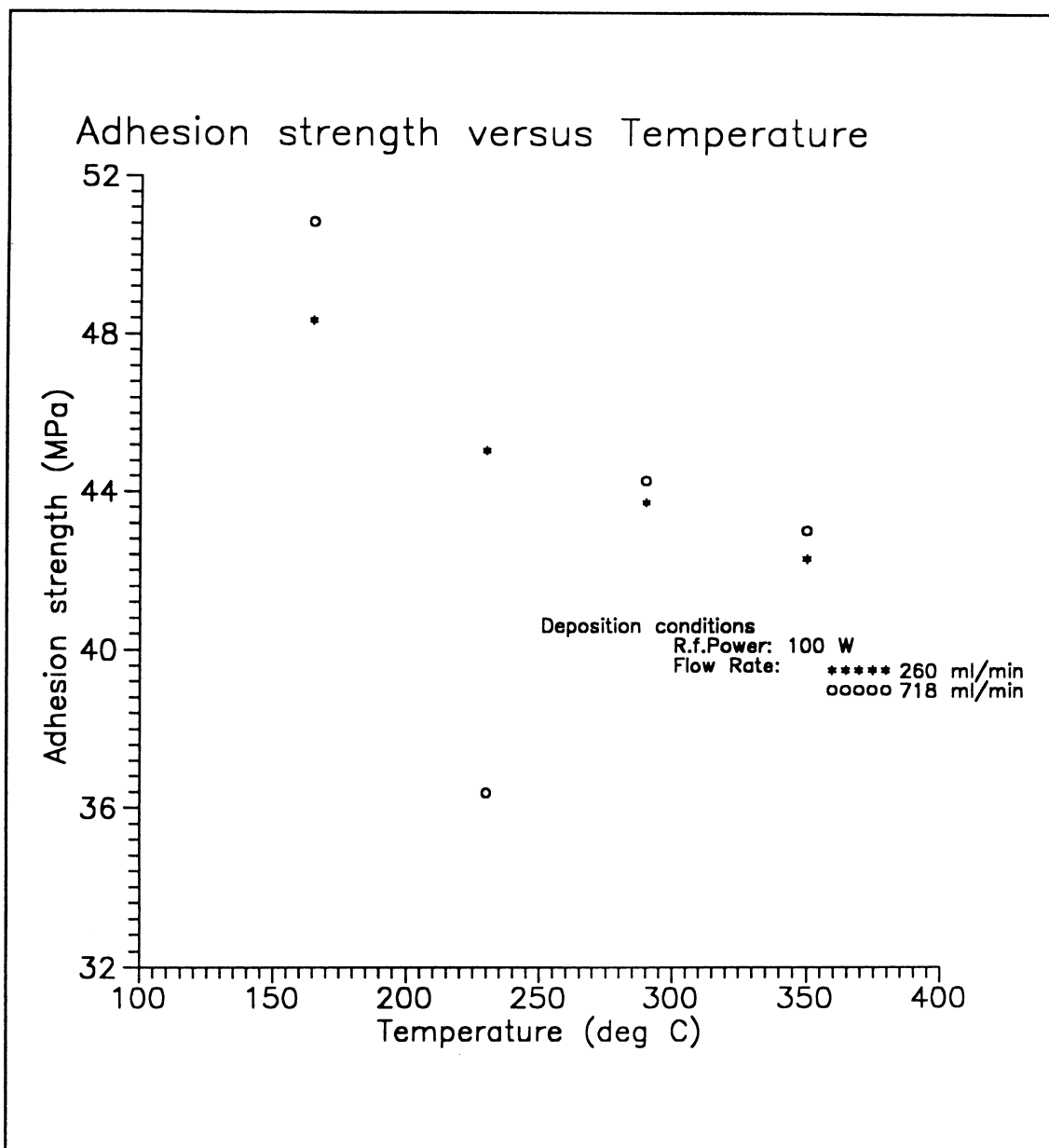


Figure 8 : Adhesion strength versus temperature at flow rates of 260 and 718 ml/min and r.f. power of 100 W

4.2.2 Adhesion strength versus flow rate

As seen in Figure 9, the film adhesion increases with increasing gas flow rates. This increase may be due to the quicker removal of gaseous species that are known to decrease adhesion by diffusing into the film surface. However, in terms of magnitude, this increase is not very large. From 41.9 MPa at 260 ml/min, the adhesion rises to around 43.4 MPa at 718 ml/min, in contrast with the almost 4 MPa variation in strength resulting from a temperature change from 165 to 350°C.

4.2.3 Adhesion strength versus film thickness

The trends displayed in the previous two sections indicated a possible relationship between adhesion strength and the deposition rate, and in turn, the film thickness. The adhesion strength for thicker films (above 3000 Å) was therefore measured. A plot of adhesion strength versus film thickness (Figure 10) however yielded ambiguous results. While the adhesion seems to be decreasing with increasing film thickness, that trend is reversed above 4000 Å. The reason for this reversal is not clearly understood and clarification is unavailable from the literature.

It may be surmised for these thicker films (> 4000Å), that a longer deposition time involved in the production of thicker films may have played a part in reducing the residual growth stresses of the film. Also, it is possible that longer deposition times

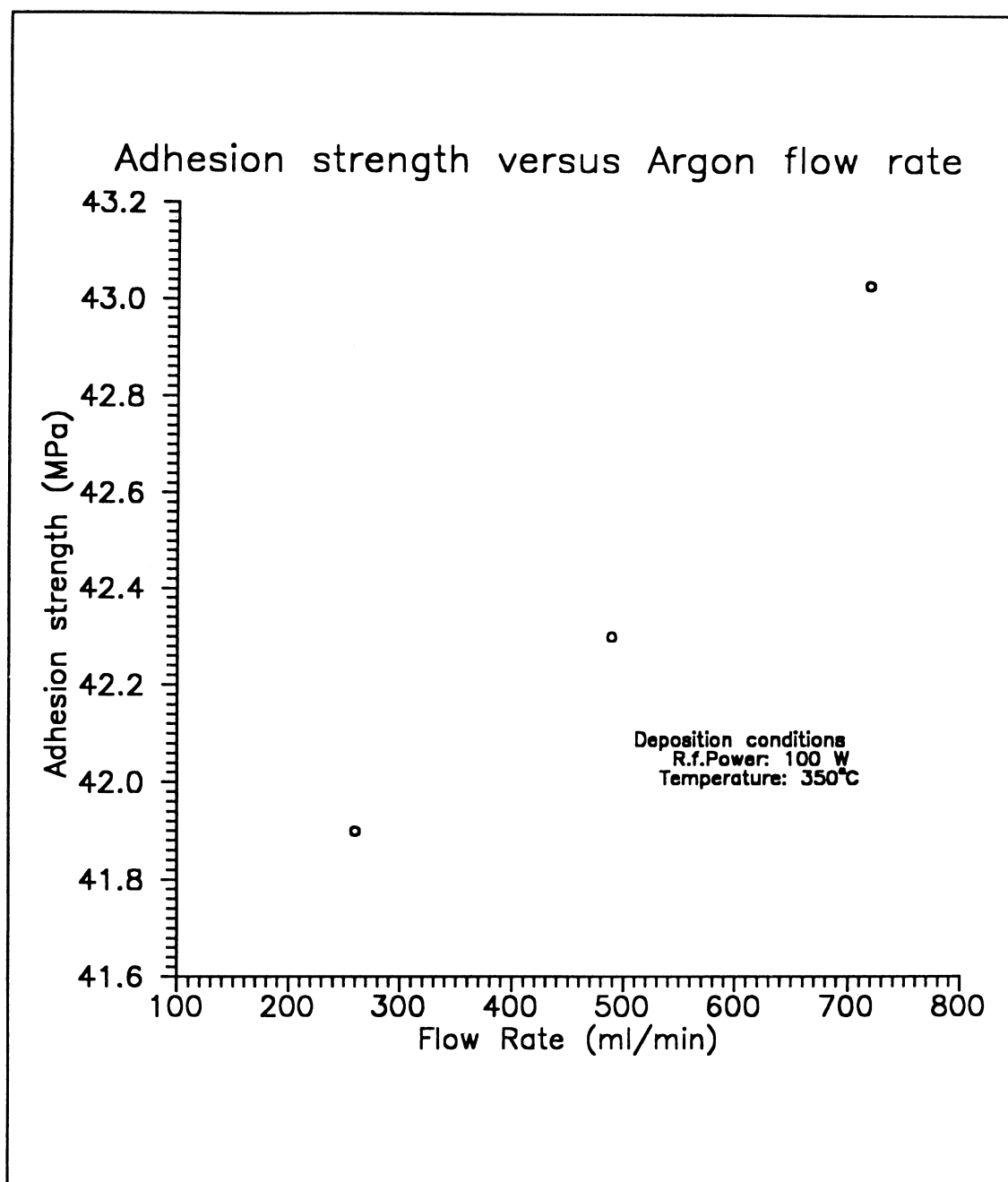


Figure 9 : Adhesion strength versus argon carrier gas flow rate at 350°C and r.f. power of 100 W

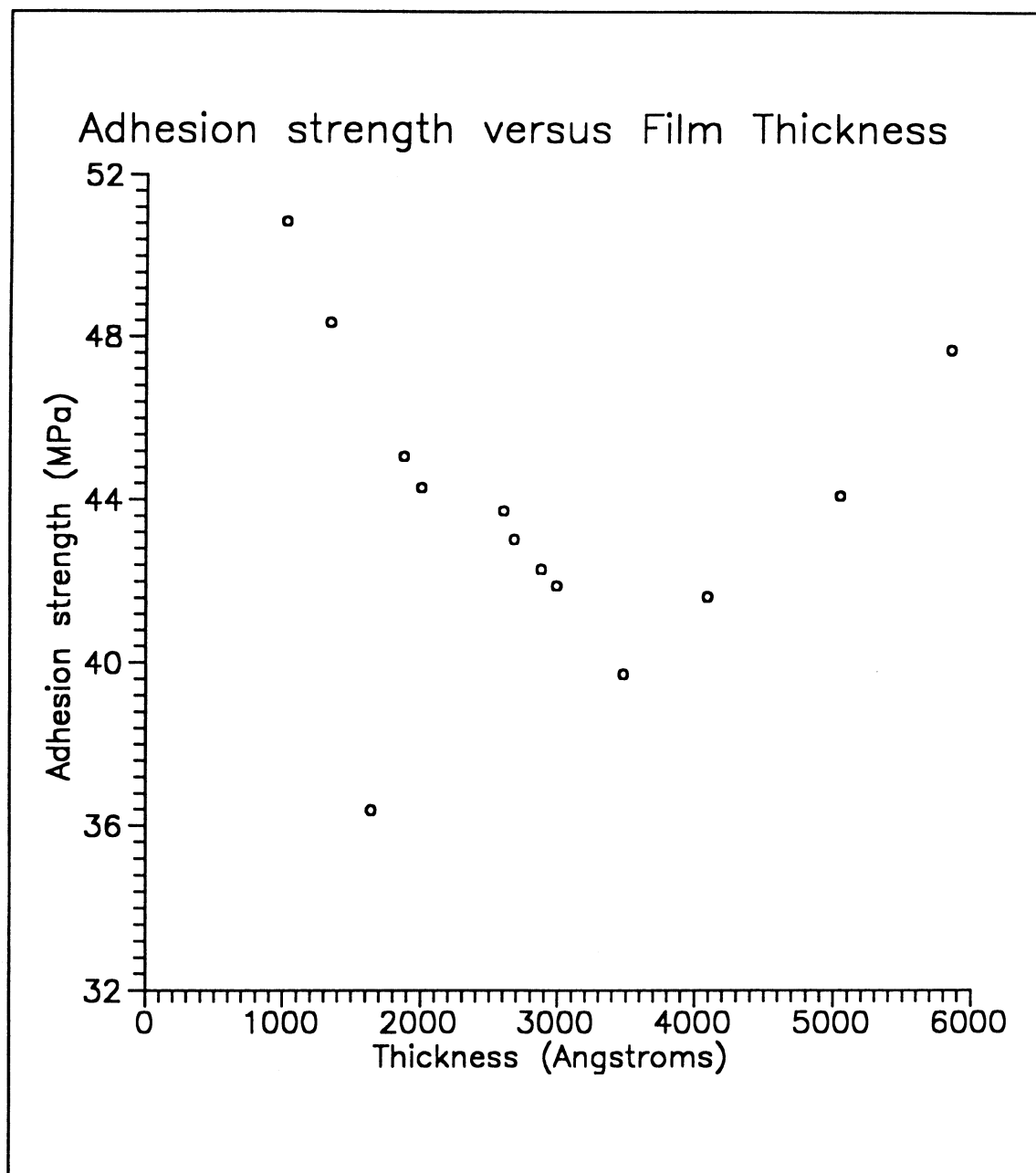


Figure 10 : Adhesion strength versus thickness

enable the devolatilization of trapped gasses such as CO, CO₂ and hydrogen from the film. Finally, as reported in literature (Mattox [1988], Neogi [1992], Sung Oh [1987]), bombardment of the surface by ions generated by the plasma over the extended deposition time may have improved adhesive properties.

4.3 Composition analysis

XPS and AES analysis was carried out on the films deposited on Si wafers at the Edwards Accelerator Laboratory at Ohio University. Shown on the following pages are the object specifications and a menu screen capture off the workstation of a sample test run of AES (Figures 11 and 12) and XPS (Figures 13 and 14).

Survey plots indicate strong peaks for silicon, carbon and oxygen, with some fluorine contamination in one sample, whose origin could not be traced. It is possible that this may have been some residual contamination from other samples in the carousel or from the testing chamber itself. The absence of fluorine in other samples makes it likely that fluorine could not have originated from the deposition reactor. The strong presence of oxygen is due to outgassing owing to the insufficient vacuum in the setup (0.15 Torr) and the presence of r.f. plasma which converts this oxygen to a highly reactive form.

Mar 14 18:08 1995 /tmp/descBAAa09057 Page 1

```

Institute:      Ohio University
Instrument:     XSAMpci
Operator:       kratos (XSAM User)
Dataset:        ~/data/FUN/Training03
Object name:    Survey-AES / 1
Date acquired:  Thu Sep 22 10:43:55 1994

Technique           = AES
Scan type           = regular
Abscissa start      = 50
Abscissa increment  = 1
Abscissa label      = Kinetic Energy
Abscissa units      = eV
Collection time     = 0.105 seconds
Ordinate label      = Intensity
Ordinate units      = Counts
# ordinate values   = 951
Cumulative etch time = 0 seconds
Object name         = Survey-AES
Gun current         = 2e-08 amps
Gun voltage         = 15000 volts
Analyser mode       = FRR
Retard ratio        = 2
Abscissa end        = 1000
Maximum sweeps     = 5
Magnification       = high
FRR code           = 4
Mag code           = 3
Detector mask       = 2
Electron Gun Mag.   = 500
Electon gun zoom    = 1
Full scale deflection = 0.32
Scans Completed     = 0
Object Aborted      = True
Acquired On        = XSAM (SAC)
Transmission Function = {
    {
        ke           = 0
        trans        = 1
    }
    {
        ke           = 5000
        trans        = 1
    }
}
Operator           = kratos (XSAM User)
Date Acquired      = Thu Sep 22 10:43:55 1994

```

Figure 11 : Object specifications for a sample AES run

Object Specification - XSAM SAC					
Technique	↻ AES	Save	Read		
Scan Type	↻ Spectrum	Submit	Done		
Title :	◆				
Excitation Parameters					
Voltage (kV)	9.000	Current (nA)	3.000		
Magnification	↻ 100 (fsd 1600.000 mm)	Zoom Factor	1.000	◆	
Analyser Parameters		Analyser Mode		↻ FRR	
Magnification	↻ high	Retard Ratio	↻ 2		
Detector Mask	<input type="checkbox"/> 1 <input checked="" type="checkbox"/> 2 <input type="checkbox"/> 3				
Data Panel	Clear				
Channel Control	↻ Step Size	Library	↻ Off		
Element	Start eV	End eV	Step eV	Dwell (ms)	# Sweeps
SurveyAES#2	50.000	1000.000	1.000	125	5
>	◆				
State Control Parameters					
<input type="checkbox"/> Etching	<input type="checkbox"/> Multipoint Analysis				

Figure 12 : Screen capture of the object specification menu for a sample AES run

Mar 14 17:11 1995 /tmp/descBAAa07454 Page 1

Institute: Ohio University
 Instrument: XSAMpci
 Operator: kratos (XSAM User)
 Dataset: ~/data/pramod/sample-1
 Object name: XPS Sp Si 2p#2 / 1
 Date acquired: Tue Oct 25 10:23:16 1994

Technique - XPS
 Scan type - regular
 Abscissa start - 1144.4
 Abscissa increment - 0.1
 Abscissa label - Kinetic Energy
 Abscissa units - eV
 Collection time - 0.298 seconds
 Ordinate label - Intensity
 Ordinate units - Counts
 # ordinate values - 201
 Cumulative etch time - 0 seconds
 Excitation name - Magnesium
 Excitation energy - 1253.6 eV
 Object name - XPS Sp Si 2p#2
 Gun current - 0.015 amps
 Gun voltage - 15000 volts
 Analyser mode - FAT
 Pass energy - 10 eV
 Abscissa end - 1164.4
 Maximum sweeps - 10
 Magnification - high
 FAT code - 2
 Mag code - 3
 Excitation code - 4
 Filament - no_preference
 Detector mask - 2
 Regions - {
 {
 region_id - 1
 region_name - XPS Sp Si 2p
 technique - XPS
 start - 96.15
 end - 102.15
 qfactor - 0.27
 amass - 28.1
 bg_type - LINEAR
 max_iters - 50
 half_life - 0
 bg_average - 1
 no_comps - 0
 }
 }
 Full scale deflection - 6
 Scans Completed - 10
 Acquired On - XSAM (SAC)
 Transmission Function - {
 {
 ke - 0
 trans - 1
 }
 }

Mar 14 17:11 1995 /tmp/descBAAa07454 Page 2

```

}
{
  ke           = 5000
  trans       = 1
}
}
Operator      = kratos (XSAM User)
Date Acquired = Tue Oct 25 10:23:16 1994

```

Figure 13 : Object specifications for a sample XPS run

Object Specification - XSAM SAC						
Technique	<input checked="" type="radio"/> XPS			<input type="button" value="Save"/>	<input type="button" value="Read"/>	
Scan Type	<input checked="" type="radio"/> Spectrum			<input type="button" value="Submit"/>	<input type="button" value="Done"/>	
Title :	◆					
Excitation Parameters						
X-ray Anode	<input checked="" type="radio"/> Magnesium					
Current (mA)	15◆	Voltage (kV)	15.000			
Analyser Parameters			Analyser Mode		<input checked="" type="radio"/> FAT	
Magnification	<input checked="" type="radio"/> high	Pass Energy (eV)		<input checked="" type="radio"/> 10		
Detector Mask	<input type="checkbox"/> 1 <input checked="" type="checkbox"/> 2 <input type="checkbox"/> 3					
Data Panel			<input type="button" value="Clear"/>			
Energy Type	<input checked="" type="radio"/> Binding	Library		<input checked="" type="radio"/> Off		
Channel Control	<input checked="" type="radio"/> Step Size	Time Control		<input checked="" type="radio"/> Dwell Time		
Element	Start eV	End eV	Step eV	Dwell (mS)	# Sweeps	
XPS Sp C 1s#2	300.000	280.000	0.100	298	50	
XPS Sp O 1s#2	543.000	523.000	0.100	298	50	
XPS Sp Si 2p#2	109.200	89.200	0.100	298	50	
◆						
State Control Parameters						
<input type="checkbox"/> Etching						

Figure 14 : Screen capture of the object specification menu for a sample XPS run

Peaks at 104 eV for the intensity versus binding energy plot indicate a presence of SiO₂. As the deposition temperature increases, a stronger SiC peak at around 102 eV may be seen. At lower deposition temperatures, a strong C-C peak exists at around 285 eV. The existence of a double hump in the samples made at 325 and 350°C indicates the presence of both C-C and Si-C bonds. For some samples, a strong carbon peak is observed at 286 eV, which may be due to the formation of a film with Si_xC_{1-x}:H type of stoichiometry. Oxygen also shows peaks corresponding to SiO₂ at 533 eV as well as a smaller peak nearby that may correspond to H₂O. It is notable that there are no visible peaks indicating pure Si or pure C presence. XPS and AES being surface techniques, it is only the top monolayer that is being analyzed; the Si substrate is not visible in the spectrum. Figures 15 through 20 show the plots obtained from a single XPS run of a coating made at 300°C, 260 ml/min and 100 W. Outputs from two other runs may be found in Appendix III. Figure 21 is an AES survey of the same sample.

Quantitative analysis using XPS or AES is not very reliable, but the output of the XSAM system indicated the presence of a compound of the form Si_xC_yO_z, where, in atomic percents,

$$19\% < x < 25\%$$

$$36\% < y < 55\%$$

and

$$24\% < z < 41\%$$

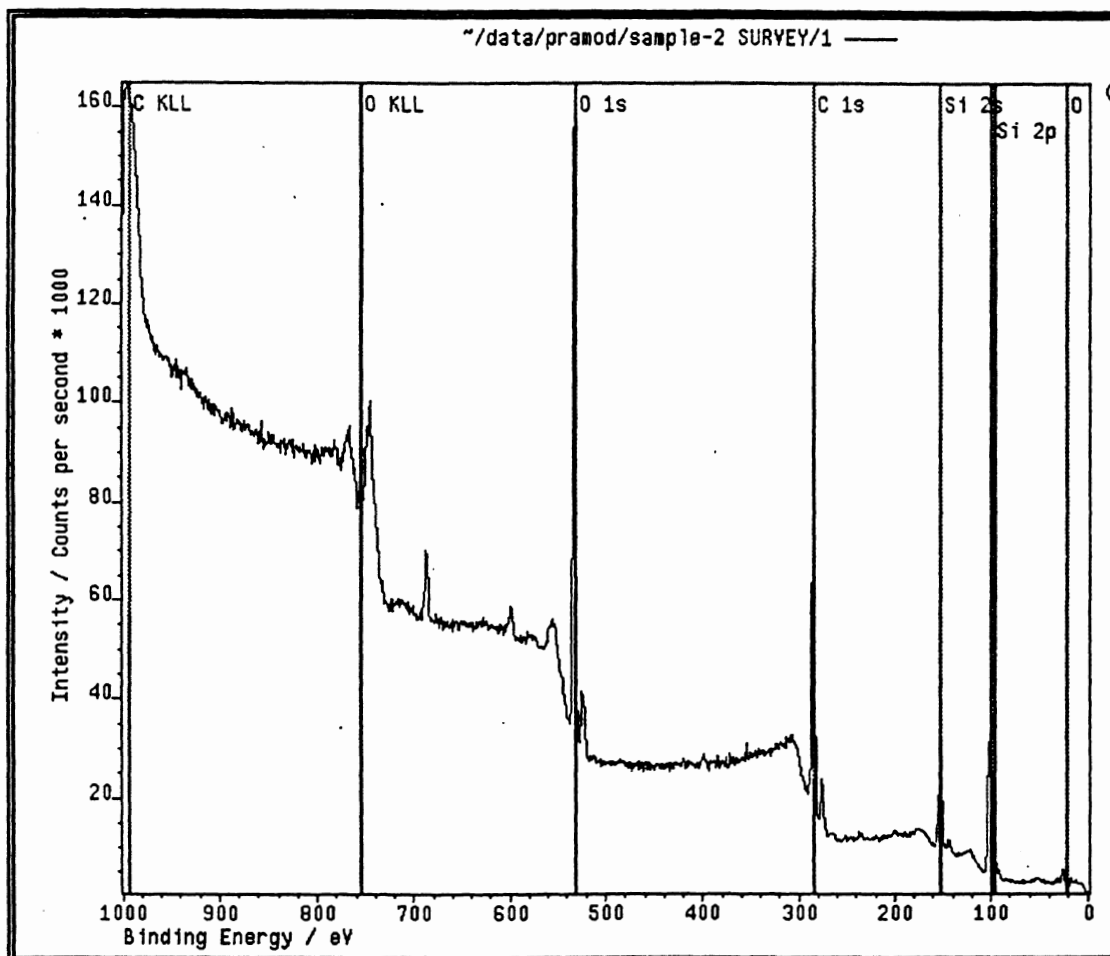


Figure 15 : XPS survey of a sample with the film made at 300°C, 260 ml/min Ar flow rate and 100 W r.f. power for 15 minutes

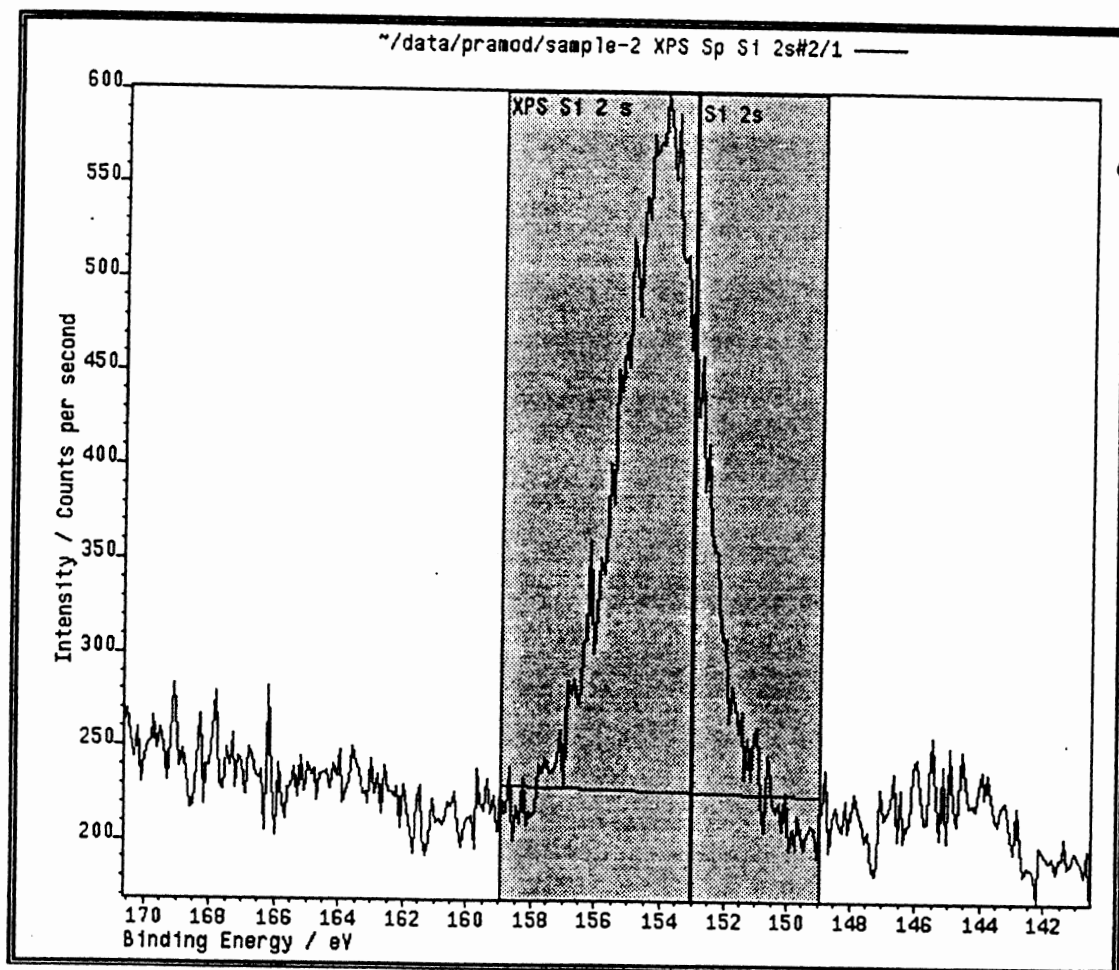


Figure 16 : Magnification of the Si 2s peak from the final XPS output for the sample
in figure 15

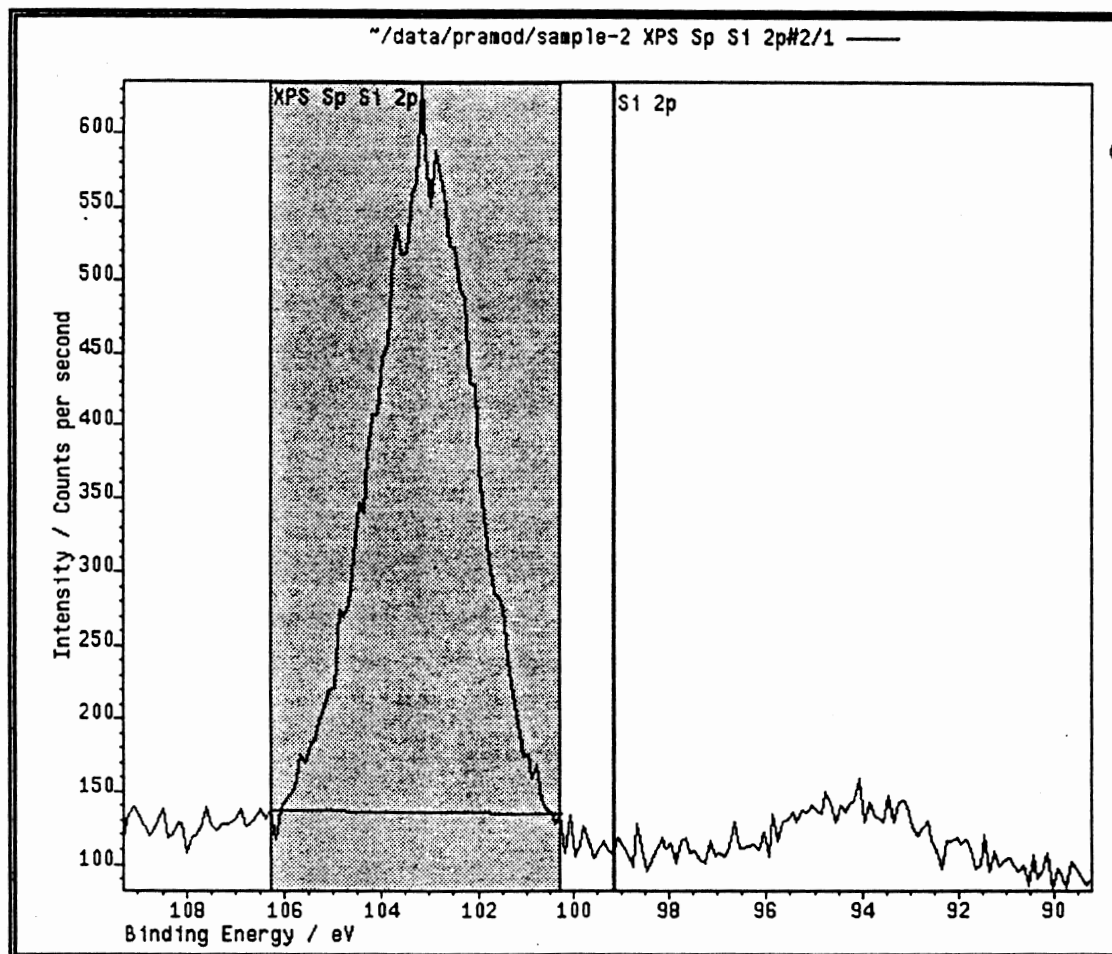


Figure 17 : Magnification of the Si 2p peak from the final XPS output for the sample in figure 15

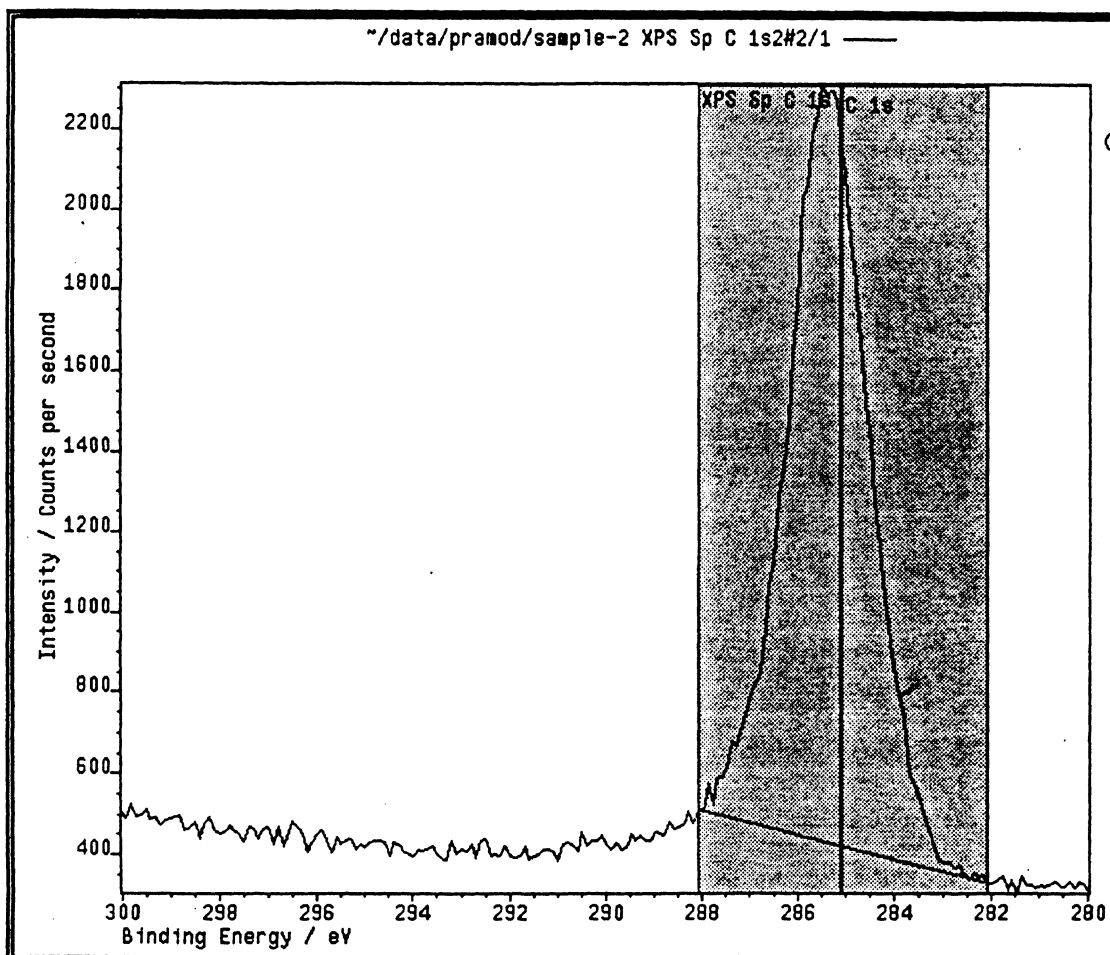


Figure 18 : Magnification of the C 1s peak from the final XPS output for the sample
in figure 15

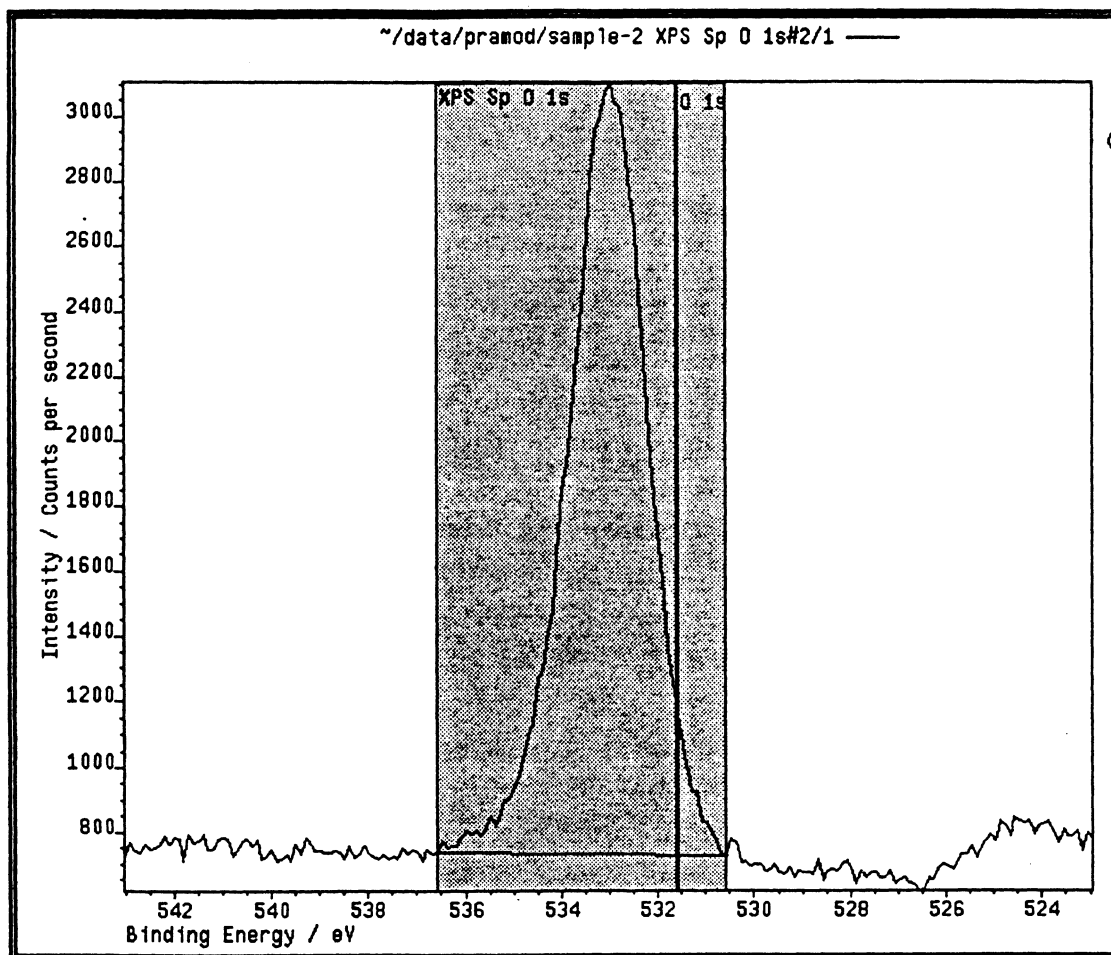


Figure 19 : Magnification of the O 1s peak from the final XPS output for the sample in figure 15

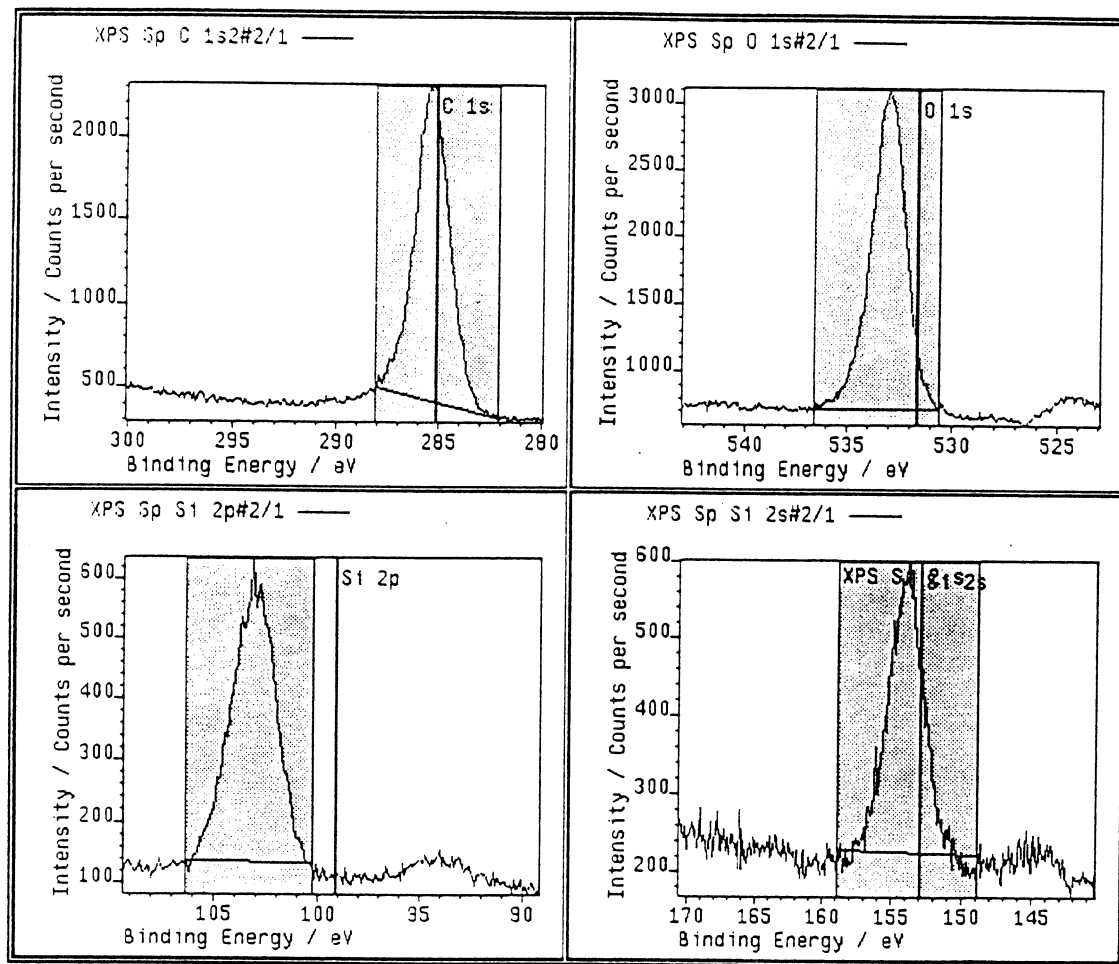


Figure 20 : Screen capture of a comparative plot of figures 16 through 19

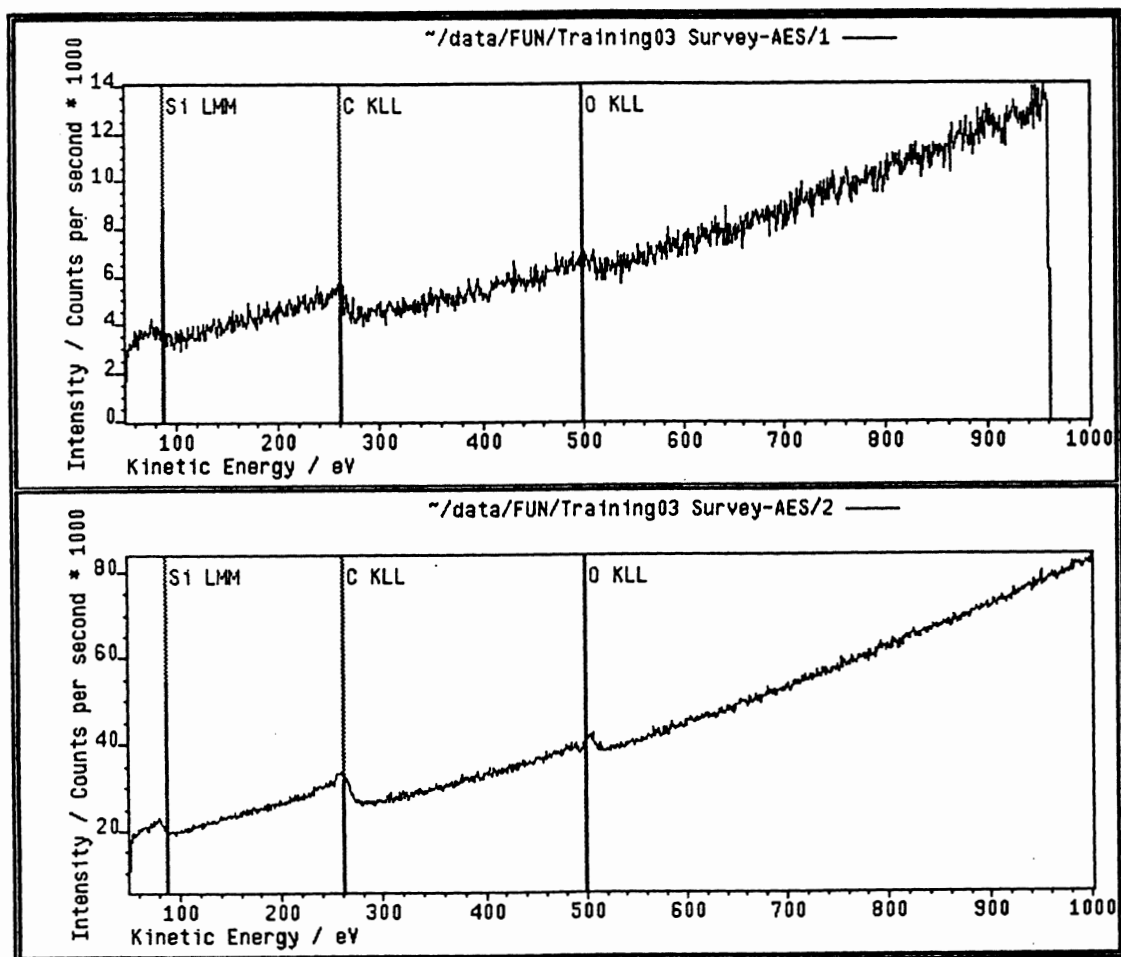
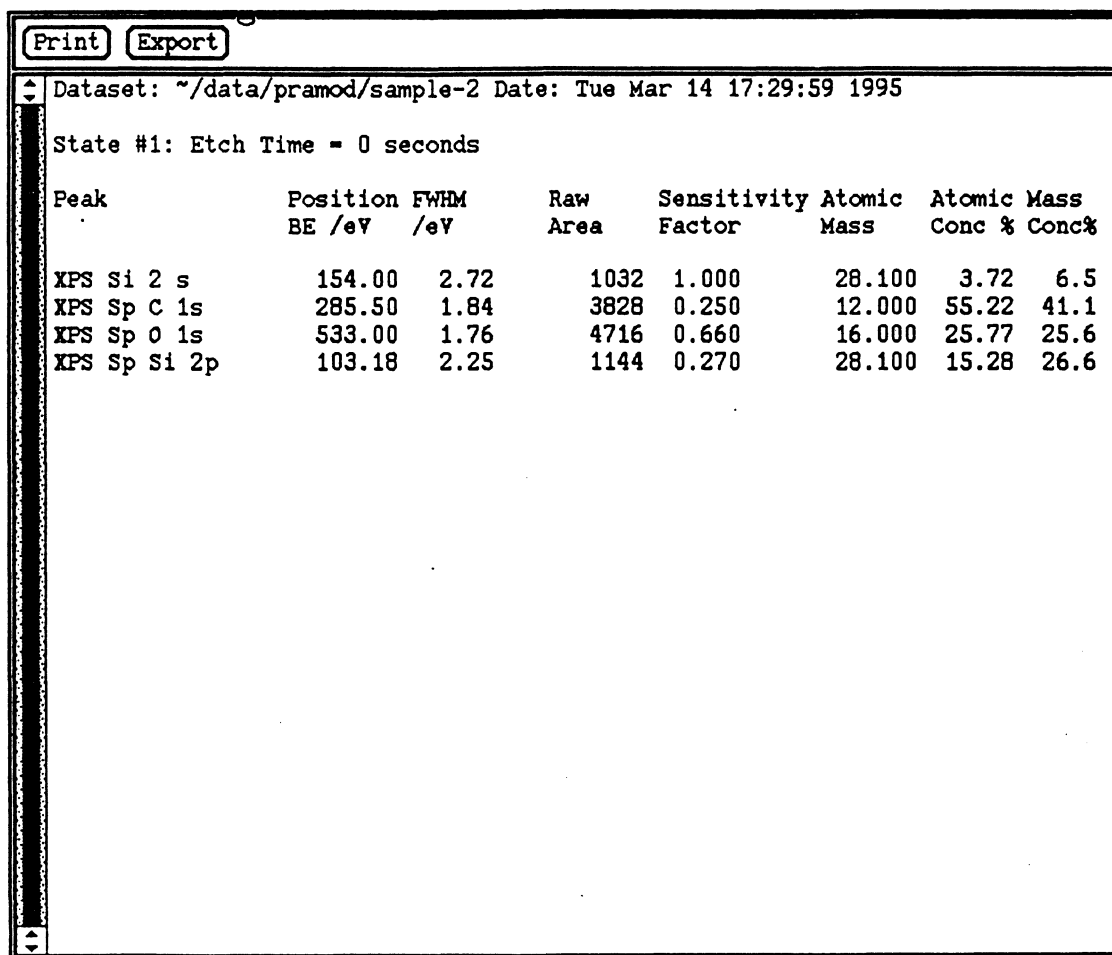


Figure 21 : AES survey of a sample with the film made at 300°C, 260 ml/min Ar flow rate and 100 W r.f. power for 15 minutes. The upper graph indicates a survey before tuning, displaying excessive noise



Dataset: ~/data/pramod/sample-2 Date: Tue Mar 14 17:29:59 1995

State #1: Etch Time = 0 seconds

Peak	Position BE /eV	FWHM /eV	Raw Area	Sensitivity Factor	Atomic Mass	Atomic Mass Conc %	Conc%
XPS Si 2 s	154.00	2.72	1032	1.000	28.100	3.72	6.5
XPS Sp C 1s	285.50	1.84	3828	0.250	12.000	55.22	41.1
XPS Sp O 1s	533.00	1.76	4716	0.660	16.000	25.77	25.6
XPS Sp Si 2p	103.18	2.25	1144	0.270	28.100	15.28	26.6

Figure 22 : Screen capture of the quantification of the data in figures 15 through 21

The output of the XSAM program for the sample whose XPS plots are seen in Figures 15 through 20, is shown in Figure 22.

This calculation by the software does not incorporate the presence of hydrogen due to the limitation of XPS and AES techniques. It is expected that a significant percentage of hydrogen exists in the film, as the breaking of the C-H bonds in the TES precursor is not complete at the low temperature and r.f. power range that this study encompasses.

To summarize, the deposited film contains a complex set of compounds involving C, H, Si and O, with SiO₂, SiC and C-C peaks clearly visible in the XPS spectra obtained. The quantitative analysis performed through XPS indicates a non-stoichiometric presence of silicon and carbon as well as a large atomic percent of oxygen.

4.4 Weight loss experiments

Polyimide composite samples coated with the deposited films were placed in an oven at a fixed temperature of 375°C and their weight measured at specified intervals. Data for times over 100 hours were not considered since the composite began to delaminate with the carbon fibers separating from the polyimide matrix. Given that there is a great deal of variability in the polyimide composite samples supplied by NASA, it is necessary to verify that the trend of weight loss in different samples is similar. This is done by plotting the percentage loss of uncoated samples; as seen in Figure 23, this

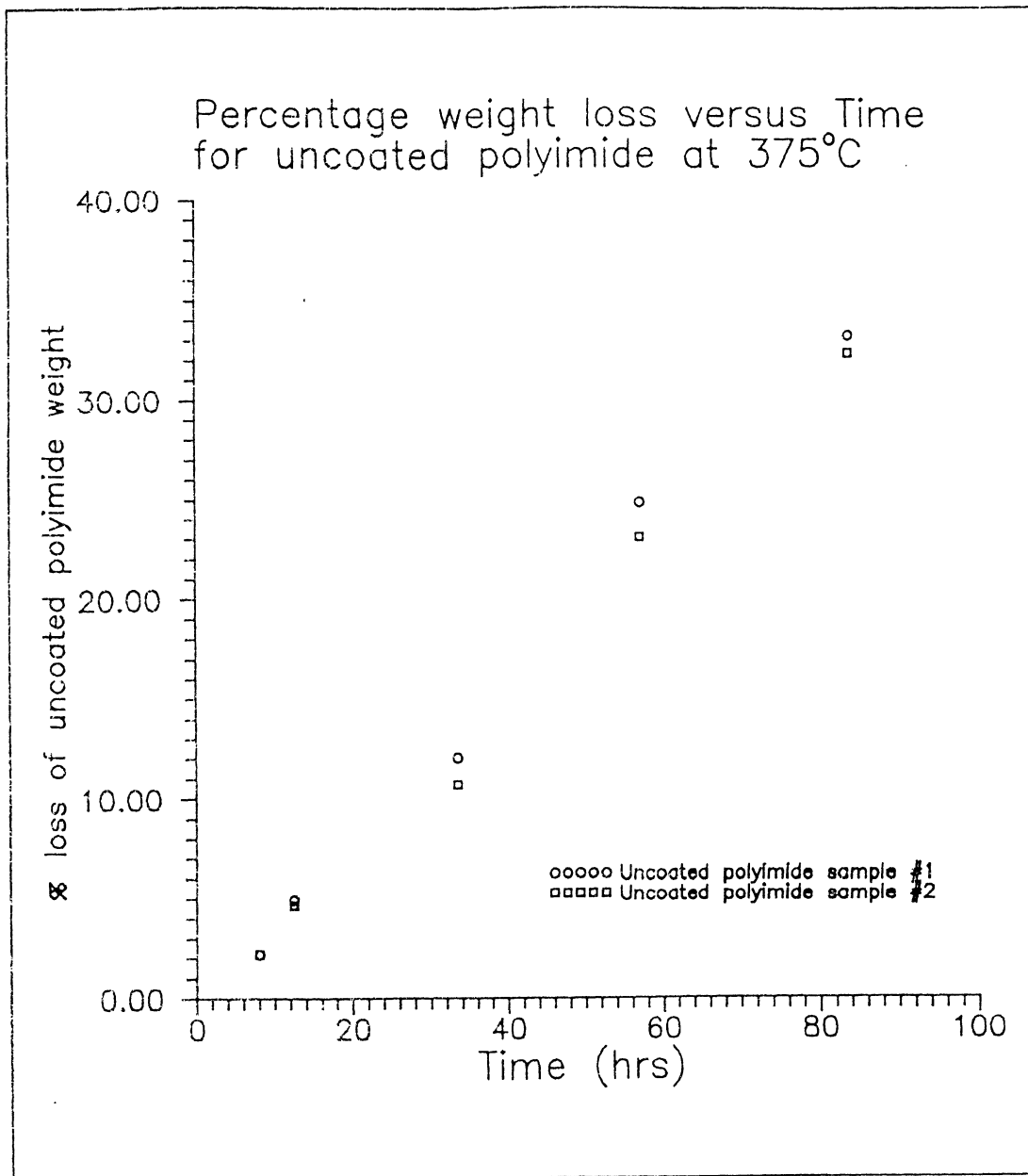


Figure 23 : Percentage weight loss versus time for two uncoated polyimide composite samples at 375°C

variation is less than 2 % for two random samples. Figures 24 and 25 show the percentage loss of coated composite samples versus time for films deposited at 260 and 718 ml/min, respectively. While the trend is similar in both cases, the absolute percentage thermo-oxidative protection is almost independent of flow rate. The effect of temperature, while slightly higher, is also less than 5 %. This indicates that film thickness or deposition rate does not change the degree of thermo-oxidative protection.

The data from the above experiments is used to ascertain the net percentage improvement in weight loss. The following expression is employed:

$$\% \text{ improvement} = \frac{\text{percent mass loss uncoated} - \text{percent mass loss coated}}{\text{percent mass loss coated}}$$

Figures 26 and 27 show the result for both sets of data. It is seen that from a maximum at around 36 hours, the percentage improvement drops rapidly to less than 15 % at 84 hours. The maximum observed protection of around 32% is in itself poor when compared to the results observed by other researchers working in the same group on other ceramic materials.

There may be many reasons for this poor result: since it is not possible to measure the actual film thickness of films deposited on composite samples or to verify their compositional nature or adhesive properties, it is possible that the nature of these films preclude oxidative protection. While the temperature at the heater surface could be measured, the temperature at the surface of the composite may have been variable and lower given that the composite has a low coefficient of heat transfer and that its thickness is around 2 mm. Secondly, in the highly reactive plasma environment during deposition,

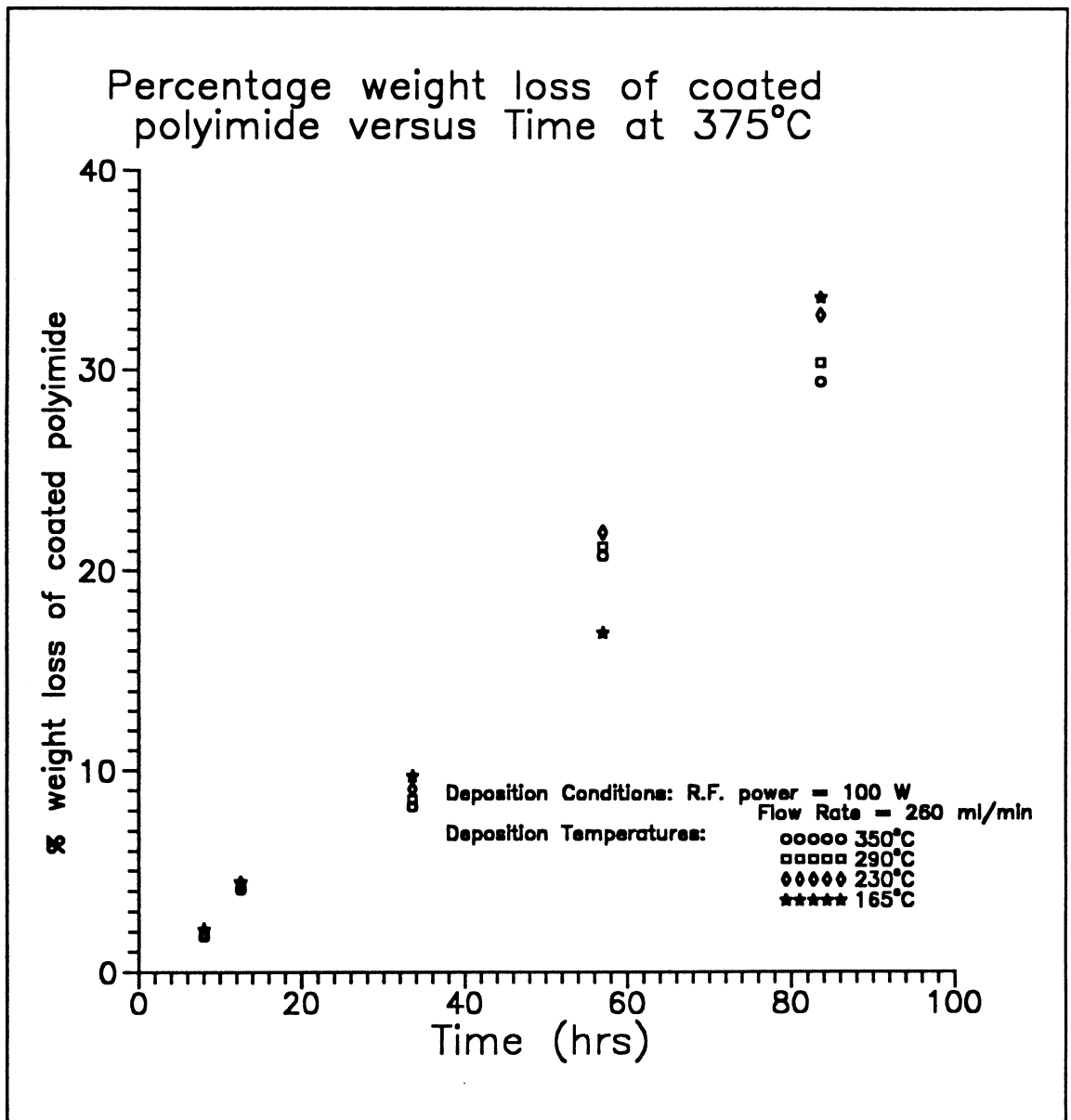


Figure 24 : Percentage weight loss versus time for coated polyimide composite at an ambient temperature of 375°C; coating conditions are: r.f. power = 100W, flow rate = 260 ml/min and temperature = 165, 230, 290 and 350°C

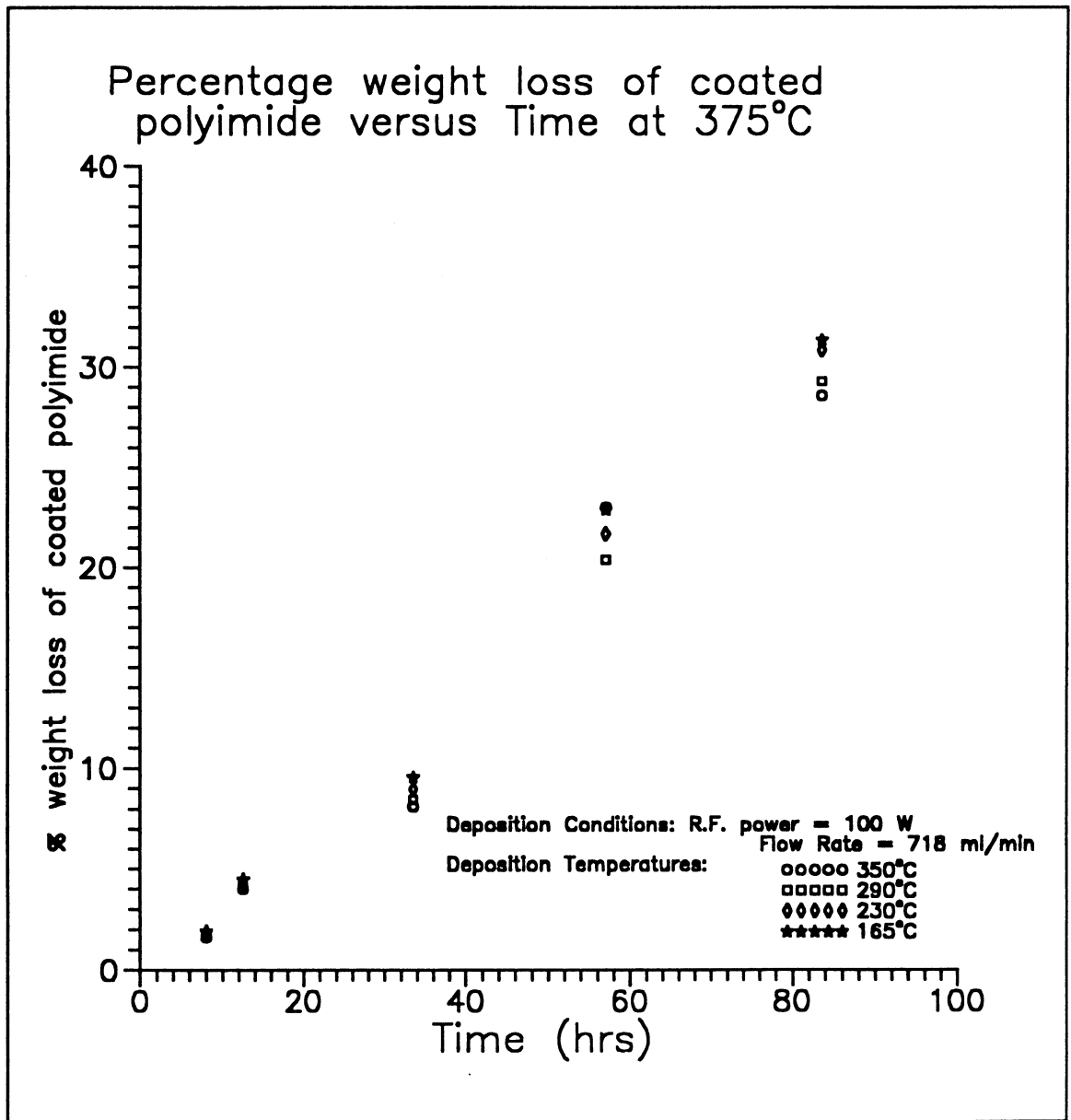


Figure 25 : Percentage weight loss versus time for coated polyimide composite at an ambient temperature of 375°C; coating conditions are: r.f. power = 100W, flow rate = 718 ml/min and temperature = 165, 230, 290 and 350°C

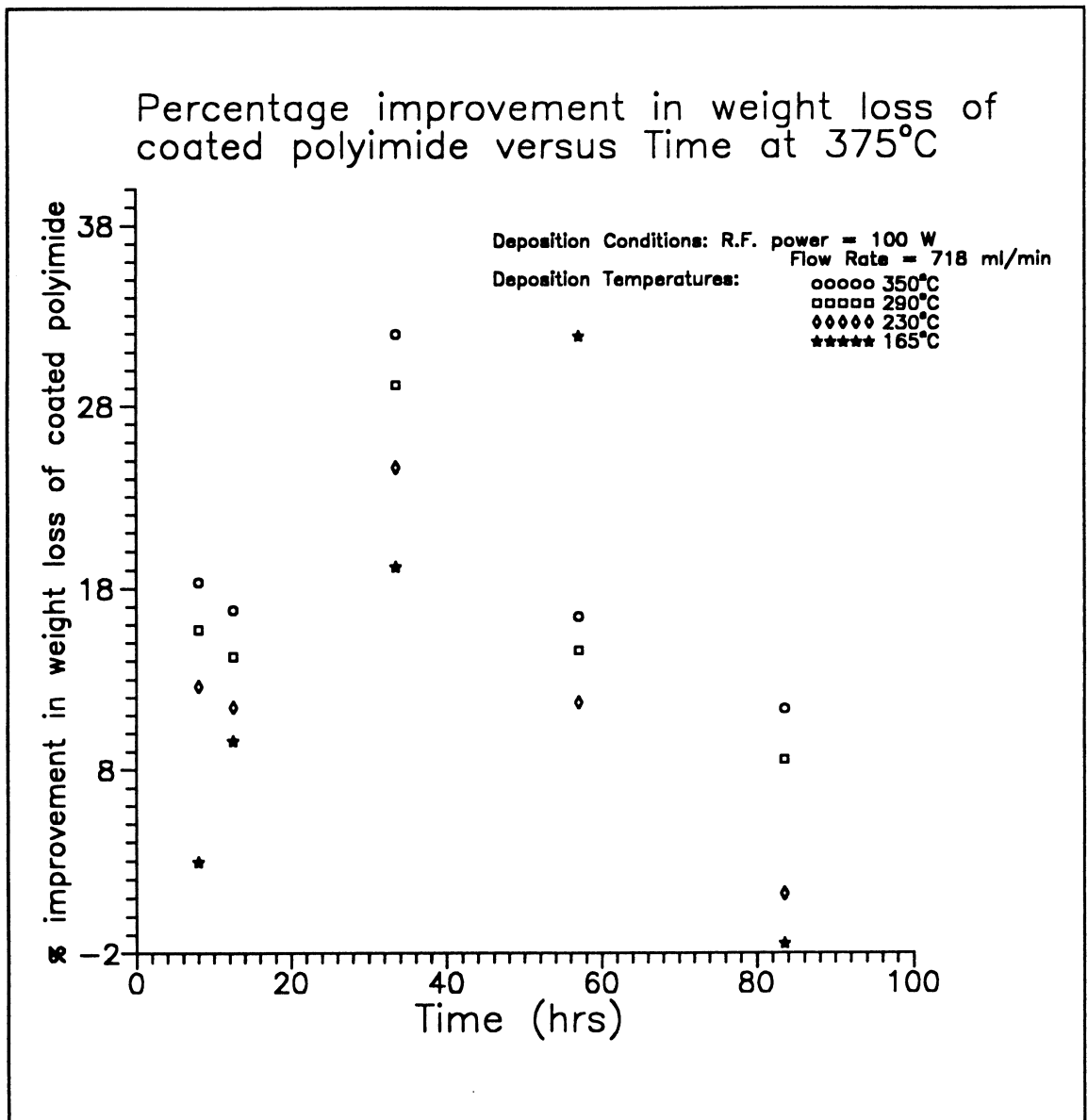


Figure 26 : Percentage improvement in weight loss versus time for coated polyimide composite at an ambient temperature of 375°C; coating conditions are: r.f. power = 100W, flow rate = 260 ml/min and temperature = 165, 230, 290 and 350°C

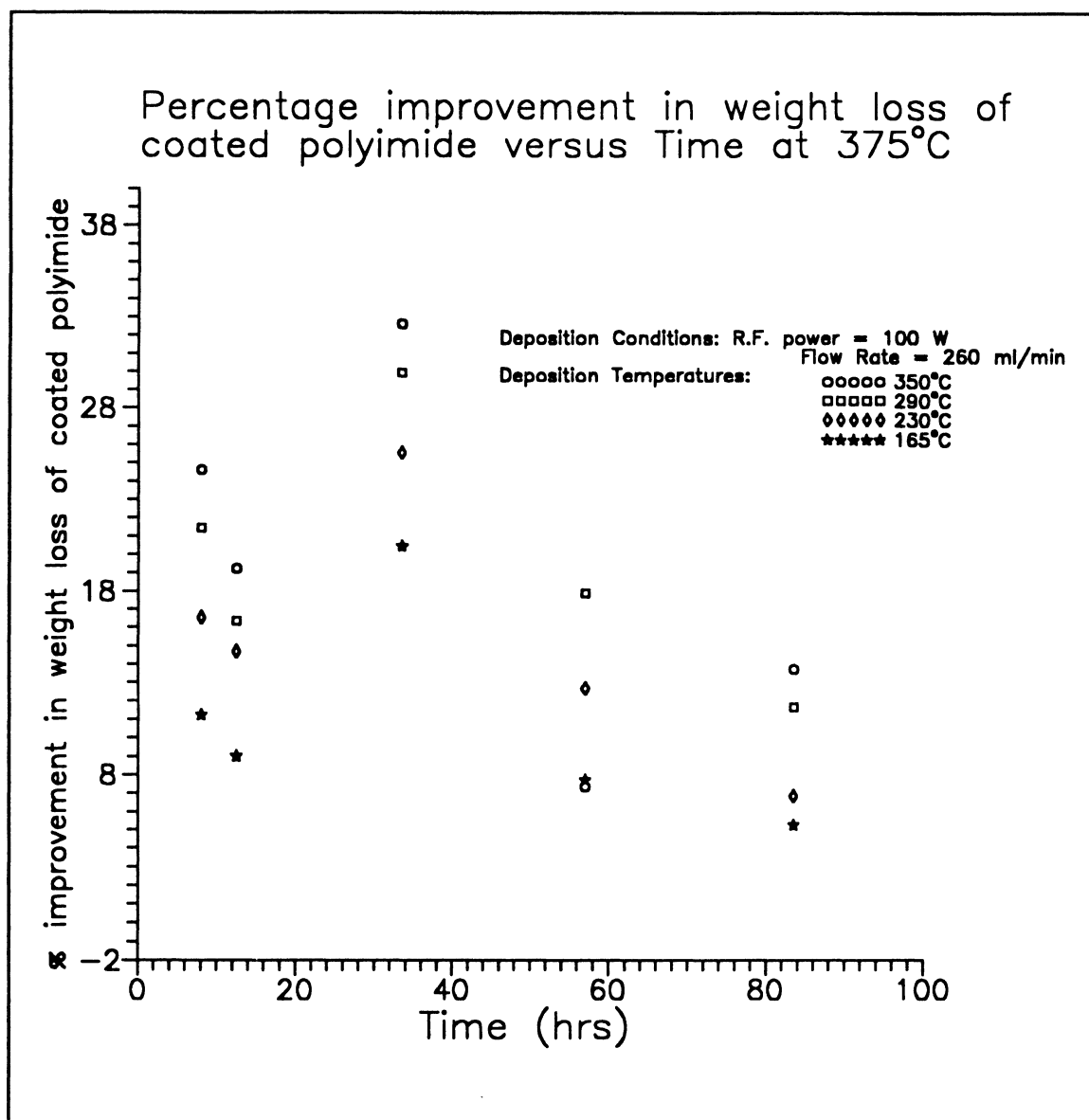


Figure 27 : Percentage improvement in weight loss versus time for coated polyimide composite at an ambient temperature of 375°C; coating conditions are: r.f. power = 100W, flow rate = 718 ml/min and temperature = 165, 230, 290 and 350°C

the presence of oxygen may have compromised the stability of the composite, thus reducing the protective threshold of the film. Thirdly, while all surfaces of the composite exposed to the precursor flow were coated, the bottom surface was hidden and may have been more susceptible to oxidation in the oven.

The raw data and calculated values used to plot Figures 23 through 27 are found in Appendix IV.

5. Conclusions

- (1). Thin film coatings have been successfully coated on silicon wafers and polyimide samples in a plasma enhanced chemical vapor deposition reactor using liquid tetraethylsilane as a precursor with argon as a carrier gas. The independent variables - substrate heater temperature, argon carrier gas flow rate and plasma radio frequency power were varied from 150 to 350°C, 260 to 718 ml/min and from 75 to 100 W.
- (2). Profilometry experiments on the deposited films show thicknesses ranging from around 950 Å to approximately 5850 Å. Adhesion strength testing of these films yielded values ranging from 40 MPa to 51 MPa.
- (3). The deposition rate, measured as the total thickness divided by the total duration of deposition, increased with an increase of substrate heater temperature.
- (4). Increasing the argon carrier gas flow rate has the effect of decreasing the deposition rate.
- (5). The deposition rate increases as the radio frequency plasma power increases from 75 W to 125 W.
- (6). Adhesion strength is generally seen to decrease as the deposition temperature is raised in the range within which tests have been conducted.
- (7). Increasing the argon gas flow rate yields films with better adhesion.
- (8). There is no definite trend for the variation of adhesion strength with film thickness; the strength is seen to generally decrease with increasing film thickness

- until approximately 4000 Å, but begins to increase again beyond this thickness.
- (9). Reproducibility in adhesion strength experiments is poor and not adequate for establishment of a conclusive trend.
 - (10). Under XPS and AES analysis, the films display the presence of silicon, oxygen and carbon; it is suspected that hydrogen is also present, though it could not be experimentally verified.
 - (11). XPS plots show the presence of SiC bonds as well as C-C and Si-O bonds. Peaks due to elemental carbon and silicon are absent. Shifts in the oxygen and carbon peaks indicate that there may be a more complex species present, involving incompletely broken C-H bonds and the reactive oxygen species present in the plasma.
 - (12). Weight loss measurements of randomly selected uncoated polyimide composite samples indicated a variability of under 2% under exposure to air at an ambient temperature of 375°C for 100 hours.
 - (13). The percentage improvement in the weight loss of coated polyimides over uncoated polyimides is taken as an index of thermo-oxidative protection. In general, this improvement is seen to increase with the thickness of the film.
 - (14). The percentage improvement in weight loss does not display a definite trend with the length of exposure to an oxidizing environment. The maximum improvement is seen after around 30 hours of exposure, after which it rapidly declines.
 - (15). The thermo-oxidative protection provided by the deposited films is poor, the best values ranging from around 19% to approximately 32% (30 hours of exposure).

6. Recommendations

- (1). A low pressure chamber should be designed whereby depositions can be carried out at a better vacuum in order to obviate the side reactions involving oxygen.
- (2). The question of flow patterns within the reactor should be studied using computational fluid dynamics simulation software such as FIDAP or ABAQUS, since this has significant import in the gas phase constituents present at the reaction surface.
- (3). Steps must be taken to model and minimize the variation of temperature along the heater surface, as this affects the reaction temperature and hence the properties of the deposited film.
- (4). In order to increase the extent of the decomposition reaction, the effect of raising the precursor temperature should be studied. It is expected that both the deposition rate as well as the stoichiometry of SiC will improve.
- (5). The problem of poor uniformity of the film must be examined. It is expected that a better precursor flow pattern and uniform heating of the substrate will remedy this. Slight plasma etching of the substrate surface before the commencement of deposition may be a favorable measure in this regard. Etching would also be expected to improve the film adhesion strength.
- (6). RBS/ERS analysis should be carried out in order that the presence of hydrogen can be detected and an accurate estimate of the atomic percent of each of the constituents become available.

References

- Beatty, Charles L., "Silicon Nitride and Silicon Carbide from Organometallic and Vapor Precursors", *Ultrastructural Processing of Advanced Structural and Electronic Materials*, 1984, Noyes Publications, Park Ridge, N.J., pp 256 - 292.
- Bielan S. and Arendt R., "Plasma-enhanced chemical vapor deposition of SiC layers using a liquid source", *Materials Science and Engineering*, 1992, v B11, pp 289 - 293.
- Chayahara A., Masuda A., Imura T. and Osaka Y., "Formation of Polycrystalline SiC in ECR Plasma", *Japanese Journal of Applied Physics*, 1986, v 25, pp L564 - L566.
- Delplancke M.P., Powers J.M., Vandentop G.J. and Somorjai G.A., "Preparation of Microcrystalline Silicon Carbide Films by Hydrogen-Radical-Enhanced Chemical Vapor Deposition Using Tetramethylsilane", *Thin Solid Films*, 1991, v 202, pp 289 - 298
- Figueras A., et al, "A morphological and structural study of SiC layers obtained by LPCVD using tetramethylsilane", *Journal of Crystal Growth*, 1991, v 110, pp 528 - 542.
- Franz, G., Kania, P. and Oelhafen, P., "Photoelectron spectroscopy of CVD diamond", *Diamond and Related Materials*, 1994, v 3, pp 1289 - 1292.

- Gopal, M., "Microwave Enhanced Chemical Vapor Deposition of Silicon Compound Thin Films and their Characterization", *M.S. Thesis*, 1991, Ohio University, Athens.
- Harding, David R., "Protective Coatings for High Temperature Polyimide Composite Materials", *Proceedings of the 4th Annual HiTemp Review*, 1991, pp 10-1 to 10-9.
- Kuhman D., Grammatica S., Jansen F., "Properties of Hydrogenated Amorphous Silicon Carbide Films Prepared by Plasma-enhanced Chemical Vapor Deposition", *Thin Solid Films*, 1989, v 177, pp 253 - 262.
- Kwatera A., "Model Studies on the Disposal of Waste Products Resulting from the Pyrolysis of CH_3SiCl_3 in CVD Process", *Ceramics International*, 1990, v 16, pp 273 - 280.
- Lorenz, H.P., "Deposition of Titanium Nitride by RF Frequency Plasma CVD", *Plasma Surface Engineering*, 1988, edited by Broszeit, E., Münz, W.D., Oechsner, H. Rie, K.-T., and Wolf, G.K., v 1, pp 15 - 34, Informationsgesellschaft Verlag, Oberursel, Germany.
- Mattox, D.M., "The Plasma Environment in Inorganic Thin Film Deposition Processes", *Plasma Surface Engineering*, 1988, edited by Broszeit, E., Münz, W.D., Oechsner, H. Rie, K.-T., and Wolf, G.K., v 1, pp 15 - 34, Informationsgesellschaft Verlag, Oberursel, Germany.
- Maury F., Mestari A. and Morancho R., "Organo-metallic Chemical Vapor Deposition of Silicon-rich Amorphous $\text{Si}_x\text{C}_{1-x}$ Refractory Layers using SiEt_4 as a Single Source", *Materials Science and Engineering*, 1989, v A109, pp 69 - 75.

- Miller, Larry M., "Plasma Enhanced Vapor Deposition of Thin Aluminum Oxide Films", *M.S. Thesis*, 1991, Ohio University, Athens.
- Neogi S., "Chemical Vapor Deposition of Silicon Dioxide Thin Films for Composite Thermo-oxidative Durability", *PhD. Dissertation*, 1992, Ohio University, Athens.
- Neogi S., Ingram D., and Gulino, Daniel A., "Improved Adhesion of Silicon Dioxide to Polyimide Composite by Ion Implantation", *Proceedings of the 4th Annual HighTemp Review*, 1991, pp 11-1 to 11-10.
- Ogbuji, Linus U.J.T., "Oxidation Instability of SiC and Si₃N₄ Following Thermal Excursions", *Journal of the Electrochemical Society*, 1991, v 138, pp L53 - L56.
- Ohring, Milton, "The Material Science of Thin Films", 1992, pp 249 - 305, Academic Press, Boston
- Satou H., Suzuki H. and Makino D., "Polyimides for semiconductor applications", *Polyimides*, 1990, pp 227 - 251, Chapman & Hall, New York.
- Schliwinski H.-J., Pelka M., Buchmann L.-M., Windbracke W., Lange P. and Cspregi L., "Stress modification and characterization of thin SiC films grown by plasma-enhanced chemical vapor deposition", *Materials Science and Engineering*, 1992, v B11, pp 73 - 77.
- Sung Oh, R., Cannon, R.M., and Richie, O.R., *Journal of the American Ceramic Society*, 1987, v 70, pp C352.
- Tanaka S. and Komiyama H., "Growth Mechanism of Silicon Carbide Films by Chemical Vapor Deposition below 1273 K", *Journal of the American Ceramic Society*, 1990, v 73, pp 3046 - 3052.

Yasui K., Fujita A., and Akahane T., "Preparation of Microcrystalline Silicon Carbide Films by Hydrogen-Radical-Enhanced Chemical Vapor Deposition", *Japanese Journal of Applied Physics*, **1992**, v 31, pp L379 - L382.

APPENDICES

Appendix I : Material Safety Data Sheet for TES



Chemists helping chemists in research & industry

aldrich chemical co., inc.
P.O. Box 355, Milwaukee, Wisconsin 53201 USA

Telephone: (414) 273-3850
TWX: (910) 262-3052 Aldrich
Telex: 26 843 Aldrich M
FAX: (414) 273-4979

ATTN: SAFETY DIRECTOR
OHIO UNIVERSITY
ATTN: DANILE GULINI
PO BOX 640
ATHENS OH 45701

DATE: 08/16/93
CUST#: 370304

M A T E R I A L S A F E T Y D A T A S H E E T P A G E 1

SECTION 1. - - - - - CHEMICAL IDENTIFICATION- - - - -

PRODUCT #: 25979-9 NAME: TETRAETHYLSILANE, 97%

SECTION 2. - - - - - COMPOSITION/INFORMATION ON INGREDIENTS - - - - -

CAS #:631-36-7
MF: C8H20SI

SYNONYMS
TETRAETHYLSILANE * TL 245 *

SECTION 3. - - - - - HAZARDS IDENTIFICATION - - - - -

LABEL PRECAUTIONARY STATEMENTS

FLAMMABLE
IRRITANT
IRRITATING TO EYES, RESPIRATORY SYSTEM AND SKIN.
KEEP AWAY FROM SOURCES OF IGNITION. NO SMOKING.
IN CASE OF CONTACT WITH EYES, RINSE IMMEDIATELY WITH PLENTY OF
WATER AND SEEK MEDICAL ADVICE.
WEAR SUITABLE PROTECTIVE CLOTHING, GLOVES AND EYE/FACE
PROTECTION.
MOISTURE SENSITIVE
KEEP TIGHTLY CLOSED.

SECTION 4. - - - - - FIRST-AID MEASURES- - - - -

IN CASE OF CONTACT, IMMEDIATELY FLUSH EYES WITH COPIOUS AMOUNTS OF
WATER FOR AT LEAST 15 MINUTES.
IN CASE OF CONTACT, IMMEDIATELY WASH SKIN WITH SOAP AND COPIOUS
AMOUNTS OF WATER.
IF INHALED, REMOVE TO FRESH AIR. IF NOT BREATHING GIVE ARTIFICIAL
RESPIRATION. IF BREATHING IS DIFFICULT, GIVE OXYGEN.
IF SWALLOWED, WASH OUT MOUTH WITH WATER PROVIDED PERSON IS CONSCIOUS.
CALL A PHYSICIAN.
REMOVE AND WASH CONTAMINATED CLOTHING PROMPTLY.

SECTION 5. - - - - - FIRE FIGHTING MEASURES - - - - -

EXTINGUISHING MEDIA
CARBON DIOXIDE, DRY CHEMICAL POWDER OR APPROPRIATE FOAM.
SPECIAL FIREFIGHTING PROCEDURES
WEAR SELF-CONTAINED BREATHING APPARATUS AND PROTECTIVE CLOTHING TO
PREVENT CONTACT WITH SKIN AND EYES.
FLAMMABLE.
UNUSUAL FIRE AND EXPLOSION HAZARDS
VAPOR MAY TRAVEL CONSIDERABLE DISTANCE TO SOURCE OF IGNITION AND
FLASH BACK.
CONTAINER EXPLOSION MAY OCCUR UNDER FIRE CONDITIONS.
EMITS TOXIC FUMES UNDER FIRE CONDITIONS.

SECTION 6. - - - - - ACCIDENTAL RELEASE MEASURES- - - - -

CONTINUED ON NEXT PAGE

France
Aldrich Chimie S.A.
9 P. 791
38191 Saint Quentin Fallavier
Cedex
Telephone: 78.46.82
Fax: 202315 Aldrich
Fax: 78946688

Japan
Aldrich Japan
Kyojima Bldg. 5th Floor
10-1, Kojimachikouen 1-chome
Chiyodaku, Tokyo
Telephone: 0337580155
FAX: 0337580157

United Kingdom
Aldrich Chemical Co., Ltd
The Old Brewery, Nine Elms
Cobham, Surrey TW9 1AA
Telephone: 0747822211
Telex: 417238 Aldrich G
FAX: 0747823779

Germany
Aldrich-Chemie GmbH & Co. KG
W-71434 Seelheim
Telephone: 06329670
Telex: 710525 Aldrich D
FAX: 0632967120/129

Spain
Aldrich Química
Avda de Cervantes 161
28 009 Alcobendas (Madrid)
Telephone: 3410619977
Fax: 3410616054
Fax: 3410616056

Switzerland
Aldrich Chemie
Industriezone 75
P.O. Box 700
CH-9470 Bülach
Telephone: 05359723
FAX: 05357420

Australia
Aldrich Chemical
Unit 2
10 Amels Ave
Cairns Hill NSW 2154
Telephone: 039555977
FAX: 039555977

Belgium
Aldrich Chemie
E. Carpentier 8
B-1300 Somain
Telephone: 035991311
FAX: 035991311

Italy
Aldrich Chimica
Via Galvani, 154
20131 Milano
Telephone: 0233617370
FAX: 0238010737



chemists helping chemists in research & industry

aldrich chemical co., Inc.

P.O. Box 355, Milwaukee, Wisconsin 53201 USA

Telephone: (414) 273-3850
TWX: (910) 262-3052 Aldrich
Telex: 26 843 Aldrich MI
FAX: (414) 273-4979**M A T E R I A L S A F E T Y D A T A S H E E T** PAGE 2DATE: 08/16/93
CUST#: 370304

PRODUCT #: 25979-9 NAME: TETRAETHYLSILANE, 97%

EVACUATE AREA.
SHUT OFF ALL SOURCES OF IGNITION.
WEAR SELF-CONTAINED BREATHING APPARATUS, RUBBER BOOTS AND HEAVY RUBBER GLOVES.
COVER WITH DRY-LIME, SAND, OR SODA ASH. PLACE IN COVERED CONTAINERS USING NON-SPARKING TOOLS AND TRANSPORT OUTDOORS.
VENTILATE AREA AND WASH SPILL SITE AFTER MATERIAL PICKUP IS COMPLETE.

SECTION 7. - - - - - HANDLING AND STORAGE - - - - -

REFER TO SECTION 8.

SECTION 8. - - - - - EXPOSURE CONTROLS/PERSONAL PROTECTION - - - - -

WEAR APPROPRIATE NIOSH/MSHA-APPROVED RESPIRATOR, CHEMICAL-RESISTANT GLOVES, SAFETY GOGGLES, OTHER PROTECTIVE CLOTHING.
SAFETY SHOWER AND EYE BATH.
MECHANICAL EXHAUST REQUIRED.
DO NOT BREATHE VAPOR.
AVOID CONTACT WITH EYES, SKIN AND CLOTHING.
WASH THOROUGHLY AFTER HANDLING.
IRRITANT.
KEEP TIGHTLY CLOSED.
MOISTURE SENSITIVE
KEEP AWAY FROM HEAT, SPARKS, AND OPEN FLAME.
STORE IN A COOL DRY PLACE.

SECTION 9. - - - - - PHYSICAL AND CHEMICAL PROPERTIES - - - - -

APPEARANCE AND ODOR
COLORLESS LIQUID
BOILING POINT: 153 C TO 154 C
MELTING POINT: -82.5 C
FLASHPOINT 79 F BY:
VAPOR DENSITY: >1
SPECIFIC GRAVITY: 0.766

SECTION 10. - - - - - STABILITY AND REACTIVITY - - - - -

INCOMPATIBILITIES
STRONG OXIDIZING AGENTS
STRONG ACIDS
MAY DECOMPOSE ON EXPOSURE TO MOIST AIR OR WATER.
HAZARDOUS COMBUSTION OR DECOMPOSITION PRODUCTS
TOXIC FUMES OF:
CARBON MONOXIDE, CARBON DIOXIDE

CONTINUED ON NEXT PAGE

France
Aldrich-Chemie S.a.r.l.
8 P 151
15707 Saint Quentin Fallavier
France
Telephone: 33(0)37620
Telex: 340215 aldrich F
FAX: 33(0)37620

Japan
Aldrich Chemical
Company, Ltd.
1-10-1, Higashi
Shinjyuku
Tokyo 162
Japan
Telephone: 81(3)33417376
FAX: 81(3)33417377

Italy
Aldrich-Chemie
S.p.A. - Milano
Via Galvani, 15/A
20151 Milano
Telephone: 02/33417376
FAX: 02/33417377

Japan
Aldrich Japan
Company, Ltd.
Cytos Building
10 Kamakura-cho
Chiyodaku Tokyo
Telephone: 03(3)551111
FAX: 03(3)550111

Spain
Aldrich Química
S.A.
Apt. 40 Carretera 16.1
28100 Alcorcón (Madrid)
Telephone: 3416619977
Telex: 27100 SACS E
FAX: 3416619026

United Kingdom
Aldrich Chemical Co. Ltd
The Old Brewery, New Road
Aldershot, Hants SP8 4JF
Telephone: 0147822111
Telex: 41228 Aldchem G
FAX: 0147823779

Germany
Aldrich-Chemie GmbH & Co. KG
10124 Schöneberg
Telephone: 0307297670
Telex: 714638 Aldch D
FAX: 03072987174739

Portugal
Aldrich-Chemie
Industria, S.A.
P.O. Box 260
170470 Beja
Telephone: 05699723
FAX: 05697429

Australia
Aldrich Chemical
Units 2
10 Armitage Ave.
Case Hill NSW 2154
Telephone: 0270899977



chemists helping chemists in research & industry

aldrich chemical co., inc.

P.O. Box 355, Milwaukee, Wisconsin 53201 USA

Telephone: (414) 273-3850
TWX: (910) 262-3062 Aldricher
Telex: 26 843 Aldrich MI
FAX: (414) 273-4979**M A T E R I A L S A F E T Y D A T A S H E E T**

PAGE 3

DATE: 08/16/93
CUST#: 370304

PRODUCT #: 25979-9 NAME: TETRAETHYLSILANE, 97%

SILICON OXIDE**SECTION 11. - - - - - TOXICOLOGICAL INFORMATION - - - - -**
ACUTE EFFECTSMAY BE HARMFUL BY INHALATION, INGESTION, OR SKIN ABSORPTION.
VAPOR OR MIST IS IRRITATING TO THE EYES, MUCOUS MEMBRANES AND UPPER
RESPIRATORY TRACT.
CAUSES SKIN IRRITATION.
TO THE BEST OF OUR KNOWLEDGE, THE CHEMICAL, PHYSICAL, AND
TOXICOLOGICAL PROPERTIES HAVE NOT BEEN THOROUGHLY INVESTIGATED.

RTECS NO: VV550000

SILANE, TETRAETHYL-
ONLY SELECTED REGISTRY OF TOXIC EFFECTS OF CHEMICAL SUBSTANCES
(RTECS) DATA IS PRESENTED HERE. SEE ACTUAL ENTRY IN RTECS FOR
COMPLETE INFORMATION.**SECTION 12. - - - - - ECOLOGICAL INFORMATION - - - - -**

DATA NOT YET AVAILABLE.

SECTION 13. - - - - - DISPOSAL CONSIDERATIONS - - - - -BURN IN A CHEMICAL INCINERATOR EQUIPPED WITH AN AFTERBURNER AND
SCRUBBER BUT EXERT EXTRA CARE IN IGNITING AS THIS MATERIAL IS HIGHLY
FLAMMABLE.
OBSERVE ALL FEDERAL, STATE AND LOCAL ENVIRONMENTAL REGULATIONS.**SECTION 14. - - - - - TRANSPORT INFORMATION - - - - -**

CONTACT ALDRICH CHEMICAL COMPANY FOR TRANSPORTATION INFORMATION.

SECTION 15. - - - - - REGULATORY INFORMATION - - - - -

DATA NOT AVAILABLE

CONTINUED ON NEXT PAGE

France
Aldrich-Chemie S r.l.
27 7101
38197 Saint Quentin Fallavier
Grenoble
Telephone: 33(0)7382
Telex: 308215 ALDRICH
FAX: 33(0)7382008

Japan
Aldrich Japan
C/O Kasei Kogyo (Shanghai)
10 Kashiwanishicho
Chiyodaku, Tokyo
Telephone: 81(3)2501155
FAX: 03(3)260157

United Kingdom
Aldrich Chemical Co. Ltd
The Old Brewery, Blaxley Road
Garnons, Basing 250 4A
Telephone: 0747627711
Telex: 411226 ALDRICH G
FAX: 0747627779

Germany
Aldrich-Chemie GmbH & Co. KG
59126 Leverkusen
Telephone: 071397979
Telex: 716638 ALDRICH
FAX: 0713979779

Spain
Aldrich-Chemie S.A.
Calle del Norte 2154
Leganés (Madrid)
Telephone: 916616677
Telex: 37189 ALDRICH

Italy
Aldrich-Chemie
c/o Galvani, 154
02151 Milano
Telephone: 0223417379
FAX: 0223417379

Spain
Aldrich-Chemie S.A.
Calle del Norte 2154
Leganés (Madrid)
Telephone: 916616677
Telex: 37189 ALDRICH

Germany
Aldrich-Chemie GmbH & Co. KG
59126 Leverkusen
Telephone: 071397979
Telex: 716638 ALDRICH
FAX: 0713979779

Spain
Aldrich-Chemie S.A.
Calle del Norte 2154
Leganés (Madrid)
Telephone: 916616677
Telex: 37189 ALDRICH



chemists helping chemists in research & industry

aldrich chemical co., inc.

P.O. Box 355, Milwaukee, Wisconsin 53201 USA

 Telephone: (414) 273-3850
 TWX: (910) 282-3052 Aldricher
 Telex: 26 843 Aldrich MI
 FAX: (414) 273-4979

M A T E R I A L S A F E T Y D A T A S H E E T P A G E 4

 DATE: 08/16/93
 CUST#: 370304

PRODUCT #: 25979-9 NAME: TETRAETHYLSILANE, 97%

SECTION 16. - - - - - OTHER INFORMATION - - - - -

THE ABOVE INFORMATION IS BELIEVED TO BE CORRECT BUT DOES NOT PURPORT TO BE ALL INCLUSIVE AND SHALL BE USED ONLY AS A GUIDE. ALDRICH SHALL NOT BE HELD LIABLE FOR ANY DAMAGE RESULTING FROM HANDLING OR FROM CONTACT WITH THE ABOVE PRODUCT. SEE REVERSE SIDE OF INVOICE OR PACKING SLIP FOR ADDITIONAL TERMS AND CONDITIONS OF SALE.

COPYRIGHT 1993 ALDRICH CHEMICAL CO., INC.
 LICENSE GRANTED TO MAKE UNLIMITED COPIES FOR INTERNAL USE ONLY

France
 Aldrich-Chemie S r.l.
 8 P. 701
 18,97 Saint Quentin Fallavier
 France
 Telephone: 148.1200
 Telex: 308715 ALDRICH F
 FAX: 7494808

Italy
 Aldrich-Chemie
 Via Galvani, 114
 20151 Milano
 Telephone: 02 23417370
 Fax: 022016737

Japan
 Aldrich Japan
 Kyocho Bldg. 8th Floor
 1-8 Ebina-Aoyama
 Chiyoda-ku, Tokyo
 Telephone: 033250155
 FAX: 033730157

Spain
 Aldrich Química
 Apt. de Correos 161
 28100 Alcala de Henares (Madrid)
 Telephone: 0416519977
 Telex: 32180 LADRUR
 FAX: 361061086

United Kingdom
 Aldrich Chemical Co. Ltd
 The Old Brewery, Nine Elms
 London W8 5NF UK
 Telephone: 0707822211
 Telex: 451228 ALDRICH G
 FAX: 0747823779

Germany
 Aldrich-Chemie GmbH & Co. KG
 W-7914 Surzheim
 Telephone: 07336930
 Telex: 714630 ALDRICH G
 FAX: 073368170779

Switzerland
 Aldrich Chemie
 Industrieweg 23
 P.O. Box 200
 CH-8670 Birmensdorf
 Telephone: 052669223
 FAX: 052657430

Australia
 Aldrich Chemical
 Unit 1
 10 Arvida Ave.
 Camberley NSW 2154
 Telephone: 027099977
 FAX: 027099974

Appendix II : Specifications of Equipment used

Plasma Reactor: March Instruments Plasmod[®] with a high temperature adapter designed by NASA Lewis Research Center.

Flow Meter: Aalborg tube # 052-015T, 0-2000 ml/min.

Substrate heater control: Glas-Col PL-312 Minitrol (1500 watts, 115 volts) rheostat.

Substrate temperature measurement: Type J thermocouple connected to an Omega HHM57 digital multimeter.

Reaction chamber pressure measurement: Granville-Phillips 280 gauge controller connected to a Granville-Phillips thermocouple gauge tube # 270006-1.

Vacuum pump: Alcatel 1004AC 1/2 hp mechanical oil seal medium vacuum pump, with a displacement of 3.2 cfm and capable of pumping down to 0.05 mTorr.

Oven: Ney 2-525 Series II furnace, 1500W at 110V, 100°C - 1100°C with a heating rate of 0°C/min - 40°C/min.

Thickness Measurement: Sloan Dektak IIA

Adhesion Strength Tester: Sebastian Five-A using Z module.

Appendix III : Output from XPS analyses

Part 1 : Sample deposition conditions - 325°C, 718 ml/min Ar flow rate and 100W r.f. power for 15 minutes

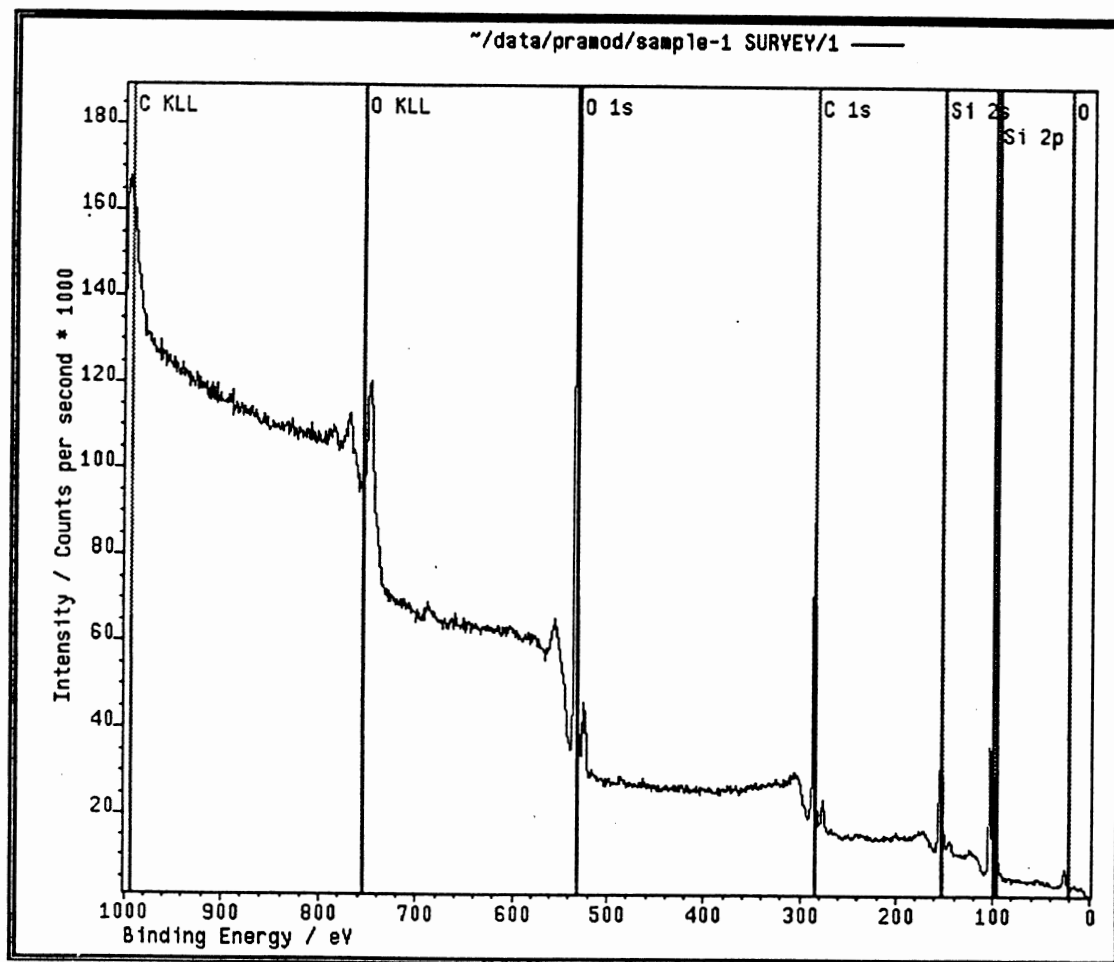


Figure A1 : XPS survey of a sample with the film made at 325°C, 718 ml/min Ar flow rate and 100 W r.f. power for 15 minutes

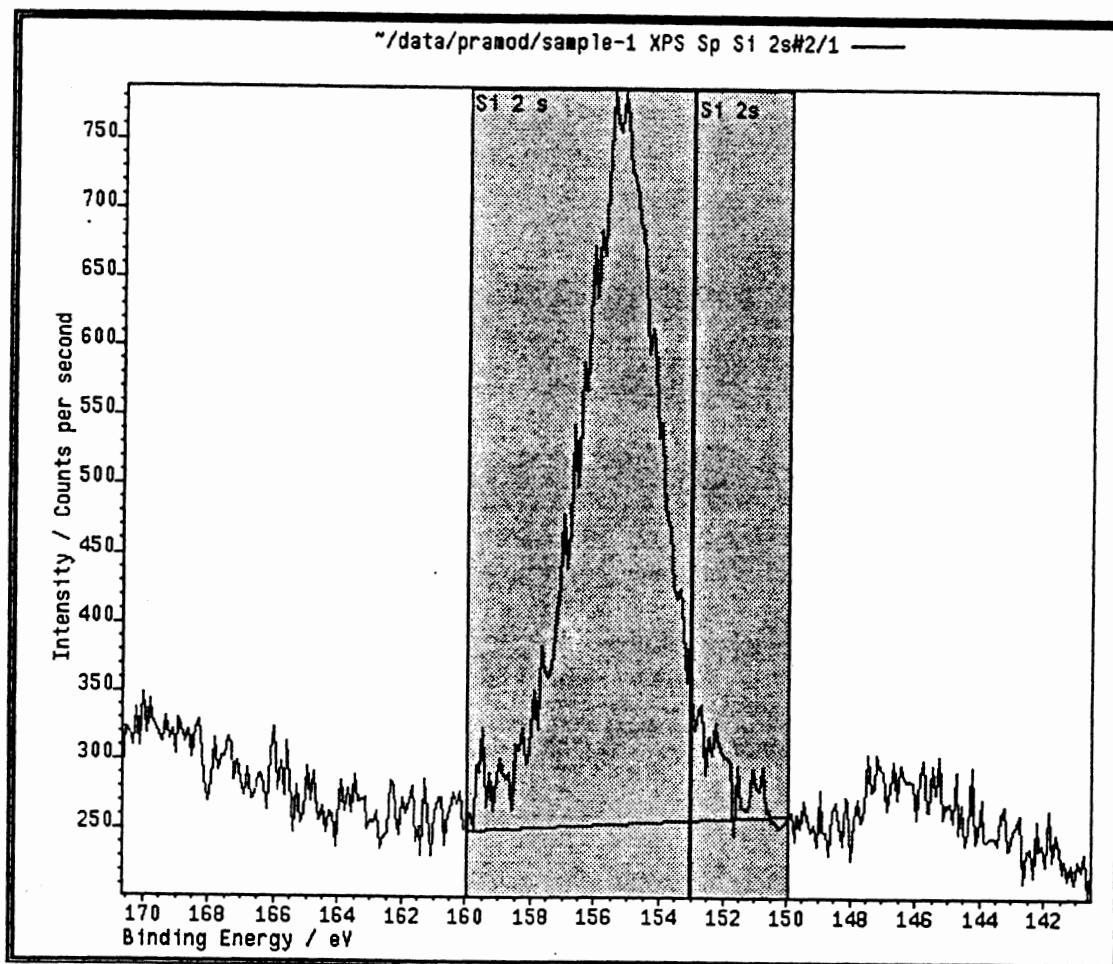


Figure A2 : Magnification of the Si 2s peak from the final XPS output for the sample
in figure A1

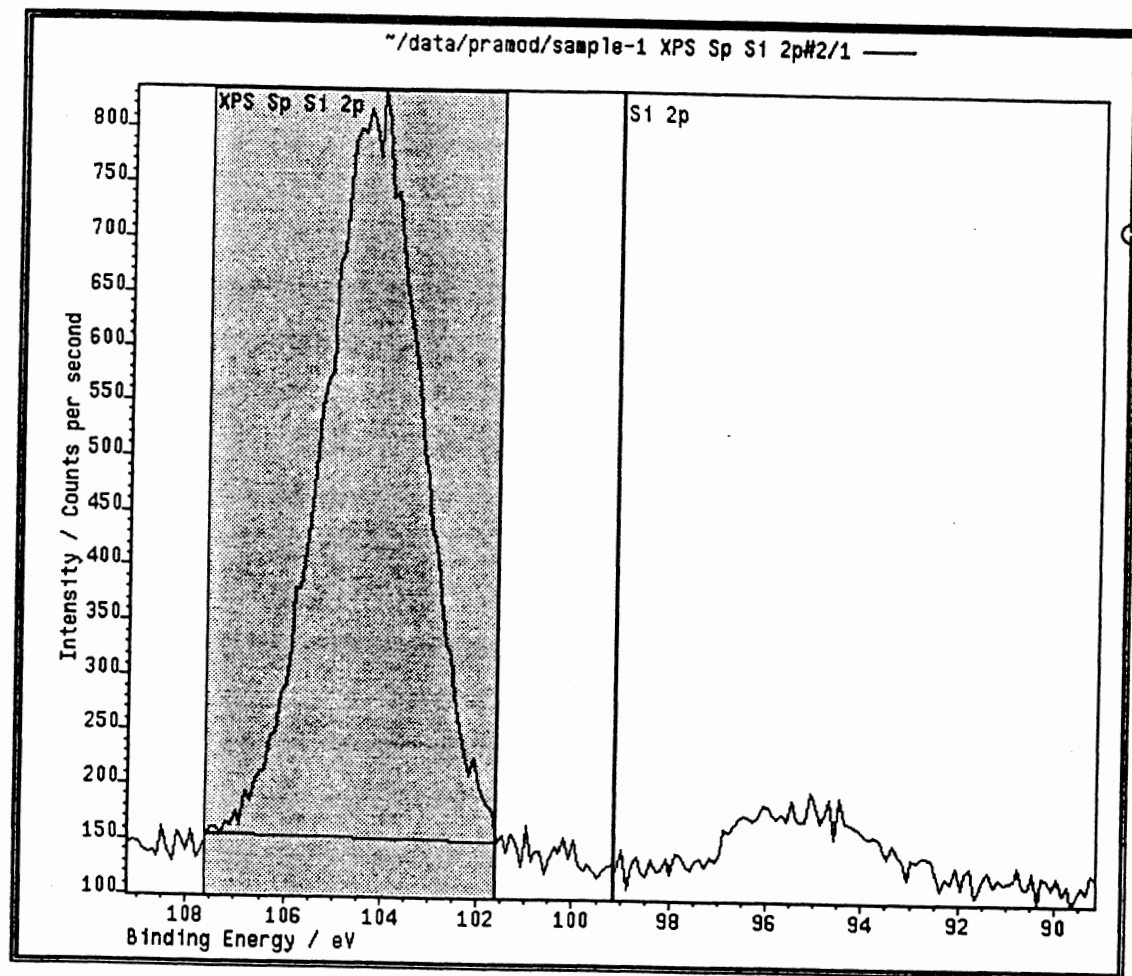


Figure A3 : Magnification of the Si 2p peak from the final XPS output for the sample
in figure A1

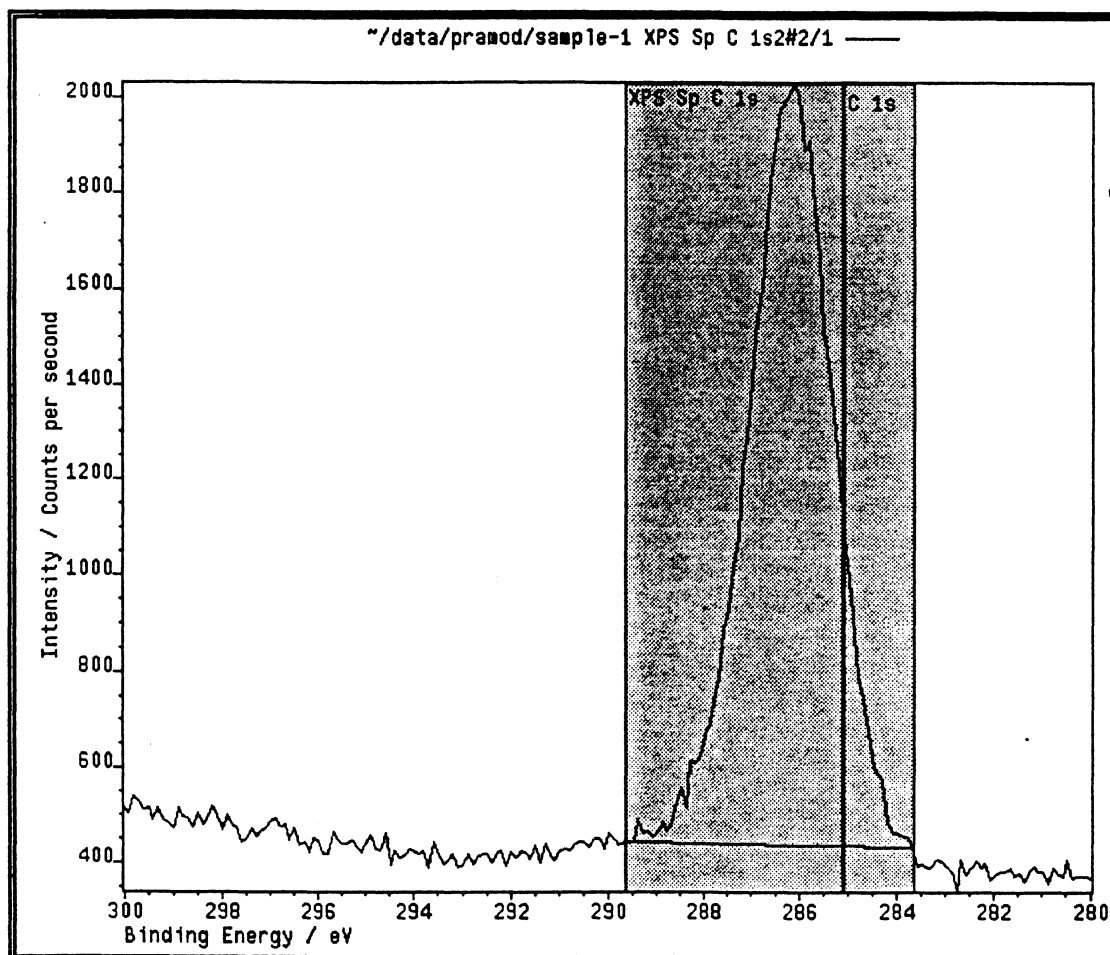


Figure A4 : Magnification of the C 1s peak from the final XPS output for the sample
in figure A1

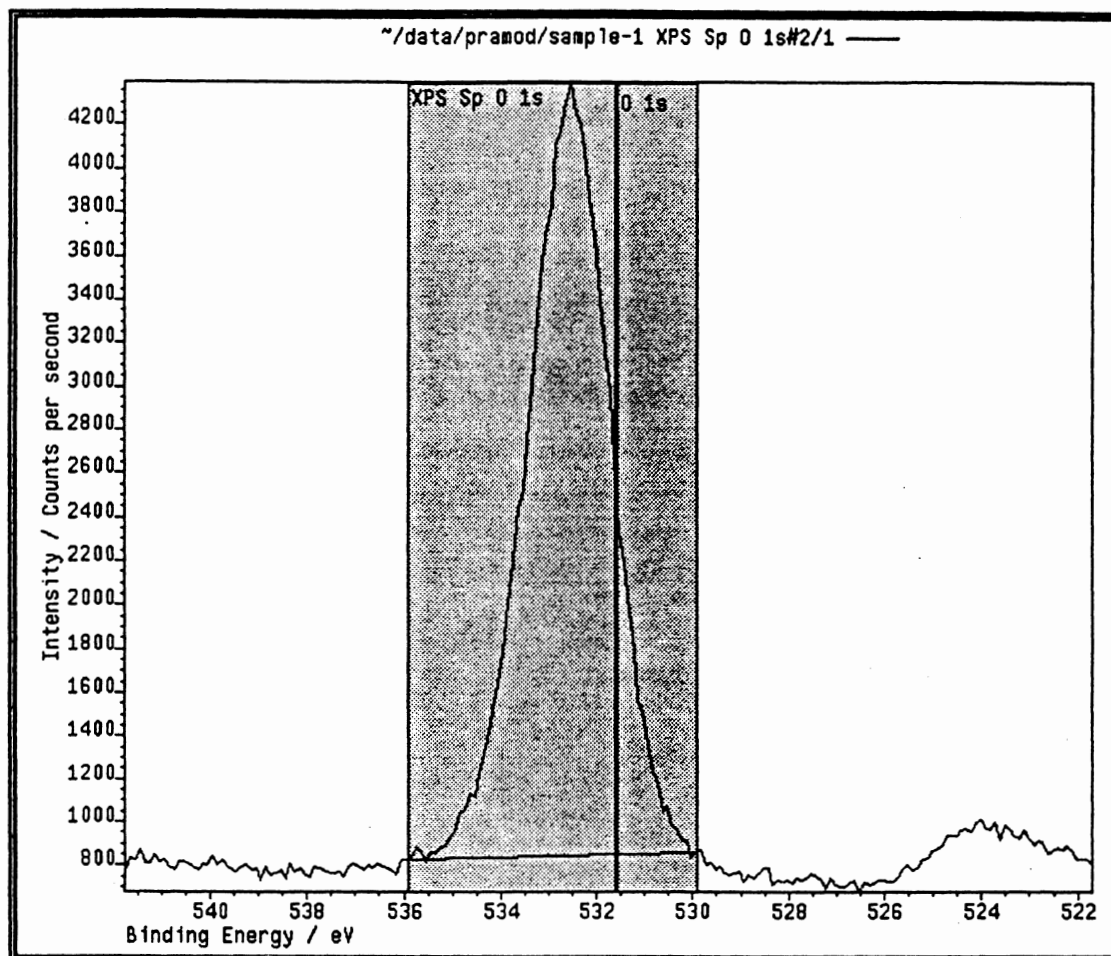


Figure A5 : Magnification of the O 1s peak from the final XPS output for the sample
in figure A1

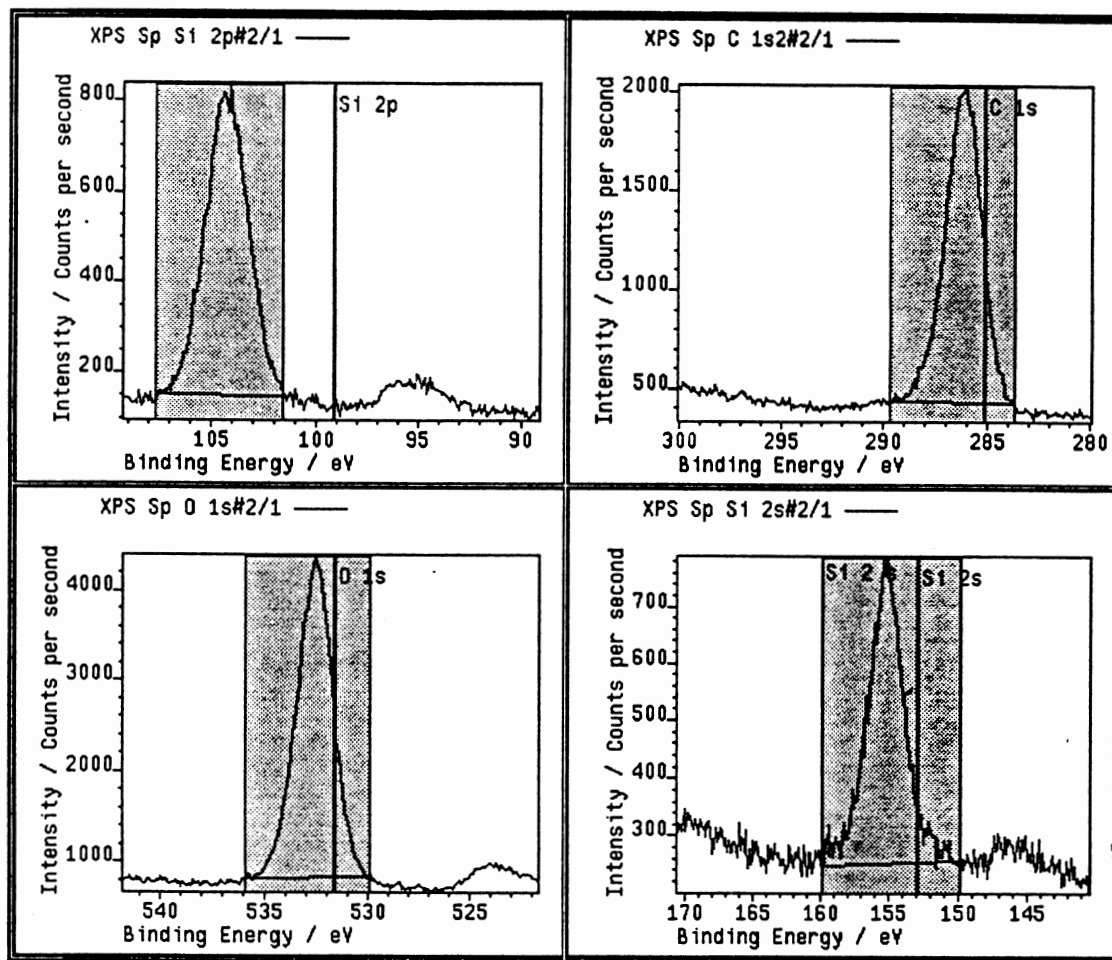


Figure A6 : Screen capture of a comparative plot of figures A2 through A5

Peak	Position BE /eV	FWHM /eV	Raw Area	Sensitivity Factor	Atomic Mass	Atomic Mass Conc %	Conc%
Si 2 s	155.50	2.61	1627	1.000	28.100	5.06	8.2
XPS Sp Si 2p	104.10	2.27	1633	0.270	28.100	18.81	30.7
XPS Sp C 1s	286.10	1.97	3356	0.250	12.000	41.77	29.1
XPS Sp O 1s	532.56	1.88	7287	0.660	16.000	34.35	31.9

Figure A7 : Screen capture of the quantification of the data in figures A1 through A6

Part 2 : Sample deposition conditions - 325°C, 489 ml/min Ar flow rate and 100W
r.f. power for 30 minutes

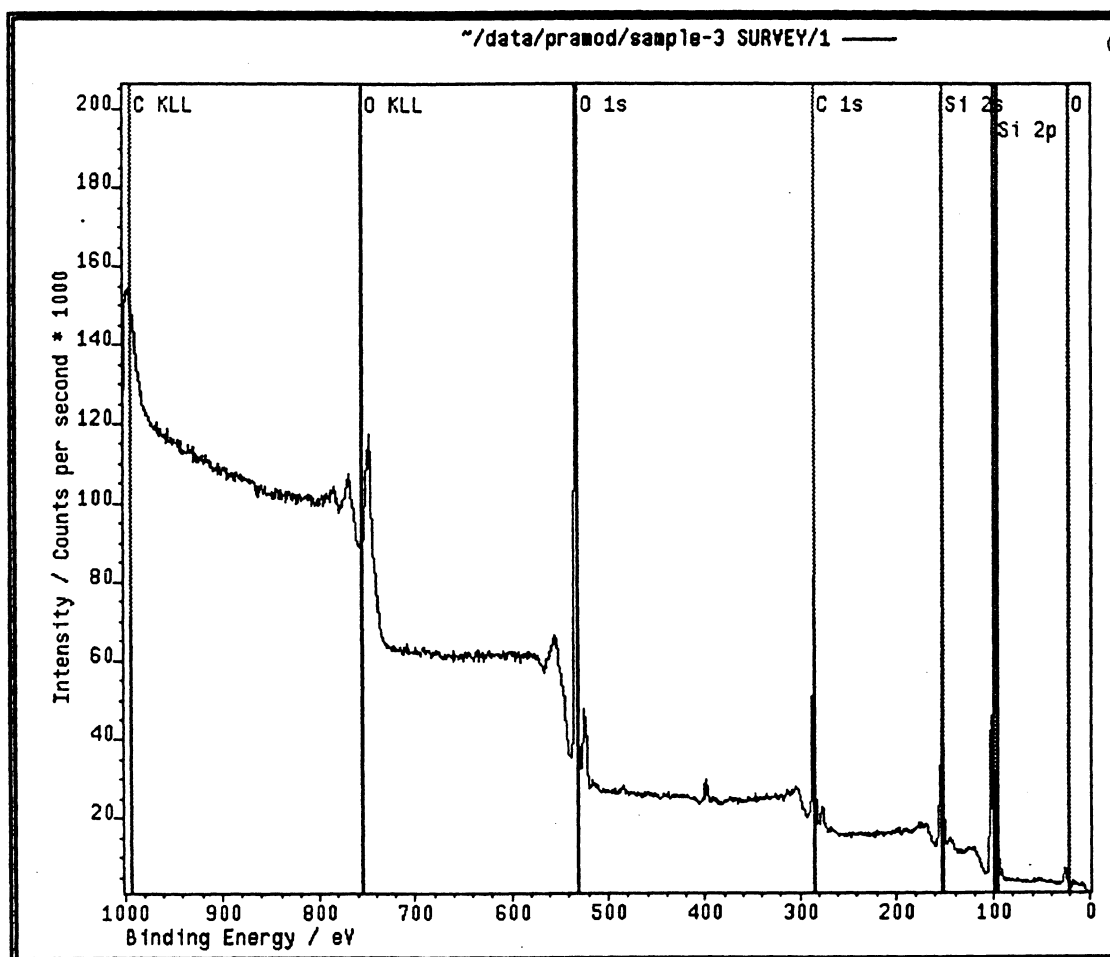


Figure A8 : XPS survey of a sample with the film made at 350°C, 489 ml/min Ar flow
rate and 100 W r.f. power for 30 minutes

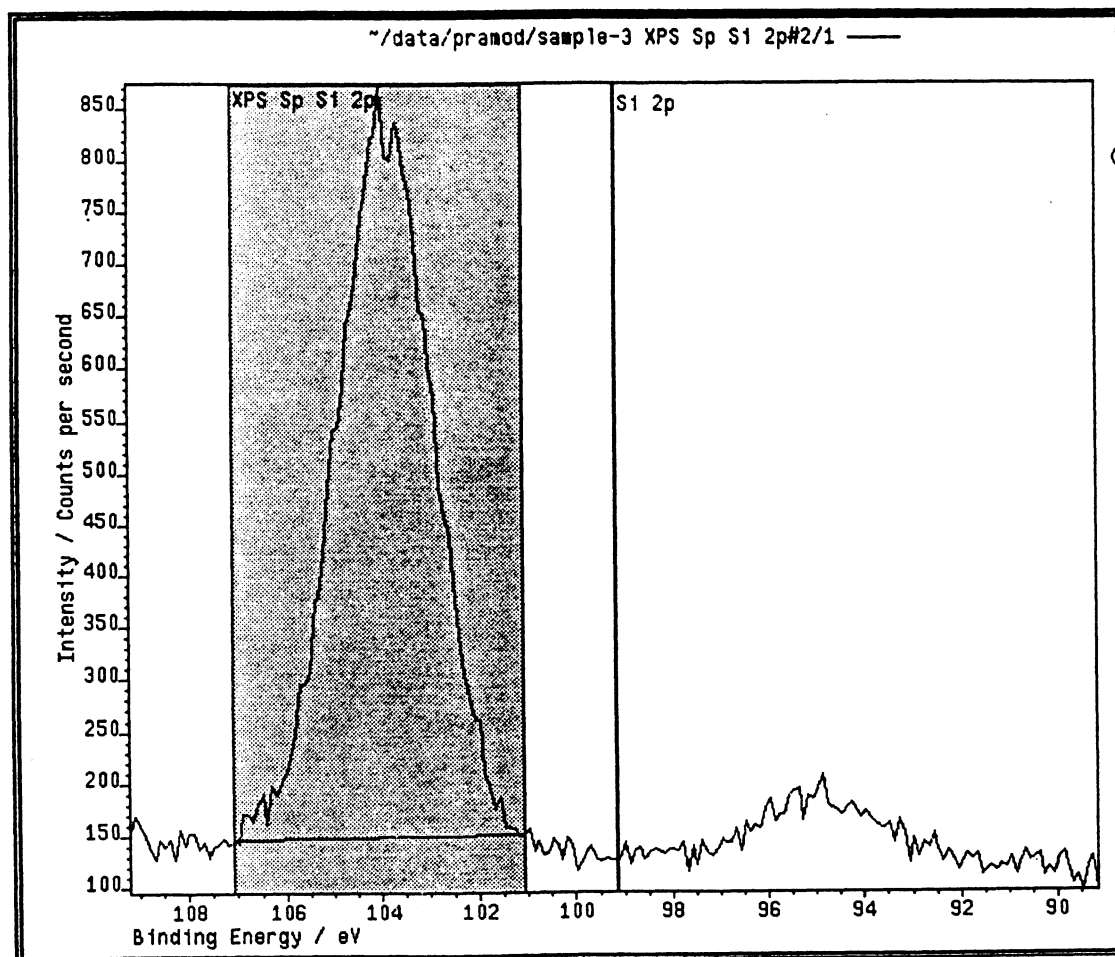


Figure A9 : Magnification of the Si 2p peak from the final XPS output for the sample
in figure A8

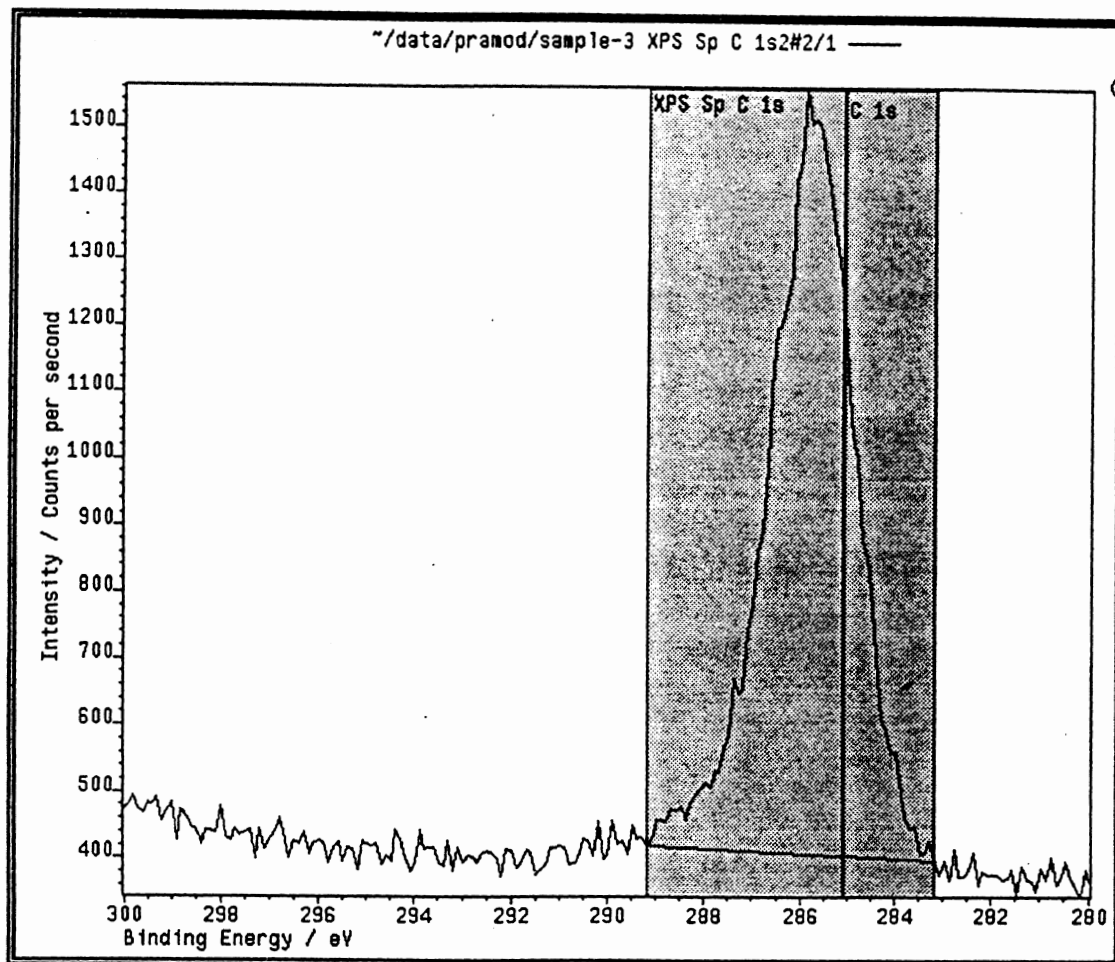


Figure A10 : Magnification of the C 1s peak from the final XPS output for the sample
in figure A8

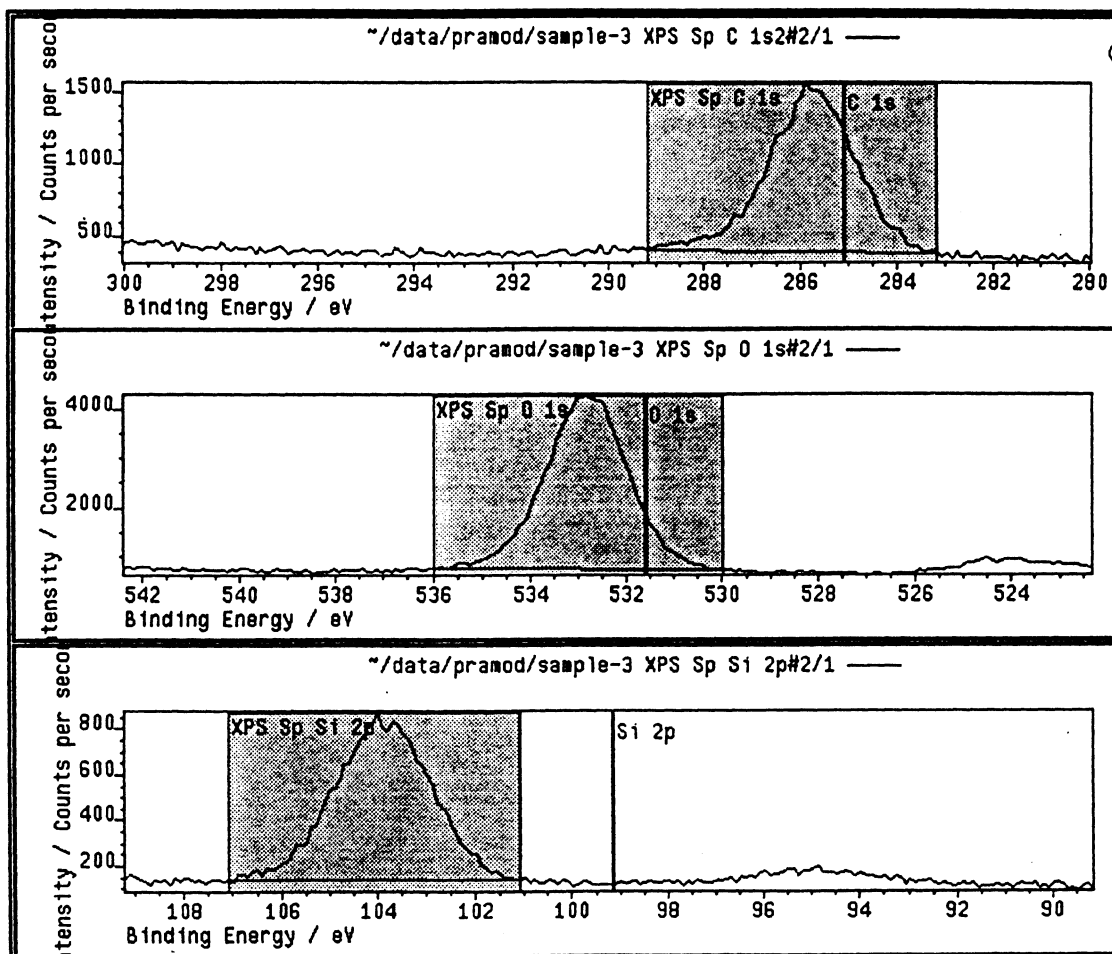


Figure A12 : Screen capture of a comparative plot of figures A9 through A11

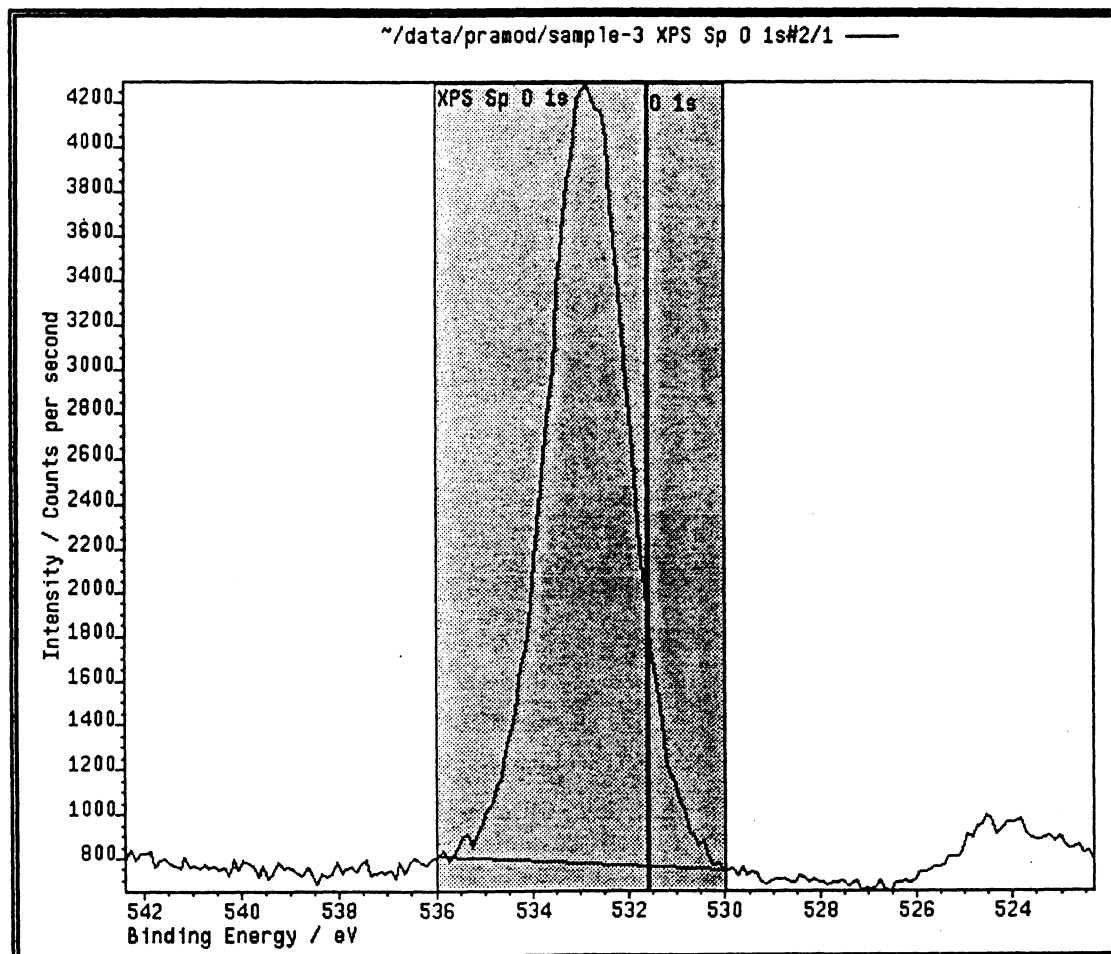


Figure A11 : Magnification of the O 1s peak from the final XPS output for the sample
in figure A8

Peak	Position BE /eV	FWHM /eV	Raw Area	Sensitivity Factor	Atomic Mass	Atomic Mass Conc %	Conc%
XPS Sp C 1s	285.90	1.93	2408	0.250	12.000	35.92	24.8
XPS Sp O 1s	532.86	1.90	7289	0.660	16.000	41.19	38.0
XPS Sp Si 2p	104.00	2.22	1657	0.270	28.100	22.89	37.1

Figure A13 : Screen capture of the quantification of the data in figures A8 through A12

Appendix IV : Polyimide composite weight loss data

Table A1 : Polyimide composite weight loss data

Time	Sample ID									
	Uncoated I	Uncoated II	5.2	5.1	6.4	6.3	10.4	10.3	10.2	10.1
0	0.3880	0.3943	0.3912	0.3629	0.3971	0.3622	0.3754	0.4010	0.3720	0.3910
8	0.3795	0.3856	0.3842	0.3562	0.3895	0.3545	0.3692	0.3941	0.3652	0.3834
12.5	0.3688	0.3759	0.3751	0.3475	0.3797	0.3460	0.3604	0.3844	0.3563	0.3734
33.5	0.3412	0.3522	0.3591	0.3319	0.3610	0.3269	0.3449	0.3671	0.3386	0.3535
57	0.2916	0.3033	0.3100	0.2859	0.3100	0.3009	0.2890	0.3192	0.2913	0.3014
83.5	0.2593	0.2670	0.2762	0.2528	0.2670	0.2403	0.2680	0.2835	0.2571	0.2682
8	2.1907	2.2064	1.7894	1.8462	1.9139	2.1259	1.6516	1.7207	1.8280	1.9437
12.5	4.9485	4.6665	4.1155	4.2436	4.3818	4.4727	3.9957	4.1397	4.2204	4.5013
33.5	12.0619	10.6771	8.2055	8.5423	9.0909	9.7460	8.1247	8.4539	8.9785	9.5908
57	24.8454	23.0789	20.7566	21.2180	21.9340	16.9244	23.0155	20.3990	21.6935	22.9156
83.5	33.1701	32.2851	29.3967	30.3389	32.7625	33.6554	28.6095	29.3017	30.8871	31.4066
8			18.3207	15.7246	12.6372	2.9590	24.6106	21.4552	16.5591	11.2743
12.5			16.8318	14.2441	11.4518	9.6149	19.2528	16.3446	14.7121	9.0367
33.5			31.9713	29.1792	24.6309	19.1999	32.6416	29.9124	25.5629	20.4866
57			16.4567	14.5999	11.7178	31.8812	7.3652	17.8961	12.6857	7.7671
83.5			11.3758	8.5353	1.2287	-1.4632	13.7492	11.6622	6.8827	5.3164